NASA
Technical
Paper
2441
C.2
AVSCOM
Technical
Report
85-B-1

May 1985

Effect of Low-Velocity or Ballistic Impact Damage on the Strength of Thin Composite and Aluminum Shear Panels

Gary L. Farley

NASA

NASA Technical Paper 2441

AVSCOM Technical Report 85-B-1

1985

Effect of Low-Velocity or Ballistic Impact Damage on the Strength of Thin Composite and Aluminum Shear Panels

Gary L. Farley

Structures Laboratory
USAAVSCOM Research and Technology Laboratories
Langley Research Center
Hampton, Virginia

National Aeronautics and Space Administration

Scientific and Technical Information Branch

Identification of commercial products and companies in this report is used to describe adequately the test materials. Use of trademarks or names of manufacturers in this report does not constitute an official endorsement of such products or manufacturers, either expressed or implied, by the National Aeronautics and Space Administration.

Abstract

Impact tests were conducted on shear panels fabricated from 6061-T6 aluminum and from woven-fabric prepreg of Du Pont Kevlar fiber/epoxy resin and graphite fiber/epoxy resin. The shear panels consisted of three different composite laminates and one aluminum material configuration. Three panel aspect ratios were evaluated for each material configuration. Composite panels were impacted with a 1.27-cm (0.50-in.) diameter aluminum sphere at low velocities of 46 m/sec (150 ft/sec) and 67 m/sec (220 ft/sec). Ballistic impact conditions consisted of a tumbled 0.50-caliber projectile impacting loaded composite and aluminum shear panels. The results of these tests indicate that ballistic threshold load (the lowest load which will result in immediate failure upon penetration by the projectile) varied between 0.44 and 0.61 of the average failure load of undamaged panels. The residual strengths of the panels after ballistic impact varied between 0.55 and 0.75 of the average failure strength of the undamaged panels. The low-velocity impacts at 67 m/sec (220 ft/sec) caused a 15- to 20-percent reduction in strength, whereas the impacts at 46 m/sec (150 ft/sec) resulted in negligible strength loss. Good agreement was obtained between the experimental failure strengths and the predicted strength with the point stress failure criterion.

Introduction

Military and commercial helicopters, like their fixed-winged counterparts, are subject to low-velocity impact damage. In addition, the military aircraft must be designed, to some degree, to be ballistic-damage tolerant.

Extensive research has been conducted on the effects of low-velocity impact damage on the tensile or compressive strength of composite laminates (refs. 1 to 5). These investigations addressed the resin and fiber characteristics that affected damage tolerance, defined the laminate failure modes, and developed methods to improve damage tolerance. The most comprehensive investigations on damage tolerance of structural elements have focused on graphite/epoxy (Gr/E) composites. These structural elements were buckling-resistant designs.

Sandwich panels fabricated from Gr/E prepreg and a honeycomb core were impacted with a metal sphere to assess their damage susceptibility (ref. 1). Tests showed that Gr/E sandwich panels were less damage resistant than S-glass/epoxy panels; an energy level one order of magnitude higher was required to sustain the same relative damage level in S-glass/epoxy. Local core crushing occurred at the impact point, and all Gr/E panels exhibited fiber fracture and permanent indentation at low energy levels.

Laminates fabricated from Gr/E and Du Pont Kevlar fiber/epoxy resin (K/E) were investigated to determine their residual strengths after being impacted at low velocity (ref. 2). Results indicate that low-velocity impact at energy levels below that necessary to create visible damage initiated catastrophic failures in all test laminates. Kevlar-graphite/epoxy (K-Gr/E) hybrid laminates were found to improve impact strength of laminates loaded in compression though not in tension.

Experimental studies to evaluate the effects of the matrix resin on the impact damage tolerance of Gr/E composite laminates are reported in reference 3. The results of mechanical property tests on neat resin show that the resin tensile properties influence the laminate damage tolerance. Furthermore, improvements in damage tolerance are not necessarily made at the expense of room temperature mechanical properties. Fiber volume fraction on the order of 40 percent may be required to provide additional improvements in damage tolerance.

The effect of low-velocity impact on the damage tolerance of composite structural elements has also been investigated. The results of an experimental investigation of low-velocity impact damage on the compression strength of Gr/E hat-stiffened panels are reported in reference 4. Panels were impacted on the skin side of the panel at both the soft unsupported skin and the stiffener location. Impact at the stiffener produced catastrophic failures at 50 to 58 percent of the design load level. The existence of local damage was found to be the significant factor in reducing the strength of the panels. Nonvisually detectable damage reduced the ultimate strength as much as extensive visually detectable damage.

Structural concepts have been devised to improve the damage tolerance of Gr/E compression panels (ref. 5). Matrix materials that fail by delamination have the lowest damage-tolerance capability. Laminates which are transversely reinforced suppress the delamination mode of failure and change the failure mode to transverse shear crippling, which occurs at a higher strain value.

Ballistic-damage-tolerance research on composite structures has concentrated on fixed-wing fighter aircraft components (refs. 6 and 7). These investigations identified the 23-mm high-explosive incendiary as the primary ballistic threat. The tolerance to ballistic impact of Gr/E and boron/epoxy composites has also been investigated (ref. 6) with 0.50- and 0.30-caliber armor-piercing projectiles. Specimen residual tensile strengths were found to be in-

dependent of the preload and the projectile velocity. Both residual strength and threshold load (the lowest load which will result in immediate failure of the specimen upon penetration by the projectile) were related to the fracture toughness of the laminates. Threshold load and residual strength of the laminates were found to be approximately 55 and 62 percent of the undamaged-panel strength, respectively.

The ballistic impact responses of metal and composites were compared in reference 7. Both metal and composites were found to lose in excess of 50 percent of their undamaged strength. Composites were found to be more resistant than metals to crack-type impact damage. Both composites and aluminum, when subjected to load, may fail on impact at applied stress levels significantly below their residual tensile strength levels. The strength loss due to small arms damage was greater in the composite panel than in metal panels.

The effects of ballistic damage on the dynamic components of helicopters were investigated (ref. 8). In this study a composite rotor hub was designed, fabricated, and impacted with a 23-mm high-explosive incendiary. Results of residual strength tests showed that the hub could withstand this type of ballistic damage.

The present investigation was conducted to understand more fully the ballistic and low-velocity damage tolerance of thin composite and thin aluminum shear panels representative of helicopter fuselage skins. The skins on the fuselage of a helicopter are generally minimum-gauge designs and develop diagonal tension fields. Three different composite laminates were studied. For the low-velocity impact tests, composite panels were impacted at no load with a 1.27-cm (0.50-in.) diameter aluminum sphere. Tests were performed with sphere impact speeds of 46 m/sec (150 ft/sec) and 67 m/sec (220 ft/sec). For the ballistic impact tests, composite panels and aluminum panels were impacted under load with a tumbled 0.50-caliber armor-piercing projectile. From the ballistic tests, the ballistic threshold load and residual strength of the panels were determined. Impact damage, failure mode, and failure location for each panel were studied. Residual strengths of the panels were compared with predicted values by means of the point stress failure criterion (ref. 9).

Experimental Procedures

Apparatus and conditions are defined in this section for all tests. The materials used to fabricate composite shear panels were Du Pont Kevlar 49 fiber/Narmco 5208 epoxy resin (K/E) and Union Carbide Thornel 300 graphite fiber/Narmco 5208 epoxy resin (Gr/E) woven-fabric prepregs. Aluminum shear panels were fabricated from 6061-T6 aluminum sheet. Three composite laminates were studied; they were $[\pm 45^{F}]_{s}$ K/E, $[+30^{F}/-60^{F}]_{s}$ K/E, and $[+45^{F}_{K}/-45^{F}_{Gr}]_{s}$ K-Gr/E hybrid. Panels with three different aspect ratios were evaluated for each material configuration: 20.3 cm × 20.3 cm (8.0 in. × 8.0 in.), 20.3 cm × 33.0 cm (8.0 in. × 13.0 in.), and 20.3 cm × 50.8 cm (8.0 in. × 20.0 in). Test conditions for the various panels are shown in tables I–IV. An improved shear fixture (ref. 10) shown in figure 1, designed to eliminate the adverse stresses in the corner of the test section of the panel, was used to test the shear panels. C-scans of selected panels were used to accurately define the damaged regions of impacted panels, and these data were compared with the visually obtained data.

Undamaged Panels

Forty undamaged shear panels were tested to failure to obtain data for comparison with data from impact-damaged panels. Panels were initially loaded at a head displacement rate of 0.05 cm/min (0.02 in/min). When the diagonal tension field was established in the panel, the loading rate was increased to 0.10 cm/min (0.04 in/min). The failure load and modes were recorded for each test.

Panels Damaged by Low-Velocity Impact

Only the composite panels were subjected to low-velocity impacts because aluminum panels are less sensitive to low-velocity impacts. The low-velocity impact test conditions are listed in table I. Test panels were not loaded when impacted because helicopters are most prone to receive low-velocity impacts when the fuselage skins are not highly stressed. Residual shear strength tests were conducted on 22 penetrated panels and 23 unpenetrated panels impacted at nominal speeds of 67 m/sec (220 ft/sec) and 46 m/sec (150 ft/sec), respectively. The panels were installed in a shear fixture, as depicted in figures 2 and 3, when impacted. A 1.27-cm (0.50-in.) diameter aluminum sphere was propelled by compressed air through a 0.50-caliber smoothbore barrel. Photoelectric cells were located at the end of the barrel to measure projectile velocity. The barrel was located approximately 7.6 cm (3.0 in.) from the test panel. All panels were impacted at a point located along a 45° line from the center of the test section of the shear panel, as shown in figure 4. Impact occurred approximately 2.5 cm (1.0 in.) from the center of the panel. This impact location was similar to the ballistic impact point. The extent of visible damage

from both low-velocity impact speeds was noted for each panel.

Panels Damaged by Ballistic Impact

Forty-five composite and aluminum shear panels were ballistically impacted with a tumbled 0.50-caliber armor-piercing projectile. The projectile is shown in figure 5. The ballistic impact tests were conducted at the U.S. Army Applied Technology Laboratory located at Fort Eustis, Virginia. The ballistic impact tests are described in tables II–IV.

The ballistic impact test apparatus is depicted in figures 6–9. A 0.50-caliber smoothbore test weapon, figure 6, was located approximately 6.5 m (21.3 ft) from the test panel, figures 7–9. Tumbling of the projectile was produced by chamfering the end of the barrel. Chamfering the end of the barrel causes a pressure imbalance on the projectile. Based upon previous tests with this apparatus, a 6.5 m (21.3 ft) distance between the weapon and test panel would produce a ¼ turn, 90° impact of the projectile. Precise control of tumbling was not achievable once the barrel of the weapon increased in temperature as a result of repeated firing. Projectile speed was determined by recording the time required for the projectile to pass through the two velocity screens, as shown in figure 8. The projectile triggered an electric photocell on each velocity screen. The screens were located 1.5 m (5.0 ft) apart.

Shear panel test specimens were assembled in the shear test fixture and portable load frame, figure 9. This assembly was positioned in front of a sand-filled pit to trap the spent 0.50-caliber projectile. Load was applied to the specimen through a hydraulically actuated displacement control load train. An impact speed of 671 m/sec (2200 ft/sec) was selected for all tests. The speed was chosen on the basis of the visual damage from 14 preliminary panel tests. In these preliminary tests, impact speeds were varied between 457 m/sec (1500 ft/sec) and 884 m/sec (2900 ft/sec). A speed of 671 m/sec (2200 ft/sec) is the expected projectile speed after traveling 366 m (1200 ft) from a weapon with a barrel 76 cm (30 in.) in length. The 366-m (1200-ft) distance is within the normal accuracy range of a 0.50-caliber weapon. The point of aim for impact was the center of the panel. Because the projectile was tumbled, precise control of the impact point was not obtainable. The actual impact point was within 5.0 cm (2.0 in.) of the aim point.

Composite and aluminum shear panels were statically loaded to various percentages of their undamaged static strength prior to being impacted. The static loads are listed in tables II–IV. The threshold load for panels of a particular material configuration and aspect ratio is defined by the panel that has the lowest average load of the preimpact load and the residual load. In this study the term residual load refers to the maximum load carried by the panel during the residual strength test. Residual strength tests were conducted on the unfailed panels. Ballistic damage, panel failure modes, and failure locations were noted for each test.

Analytical Procedures

Classical diagonal tension fields (refs. 10 and 11) were exhibited by the thin composite and aluminum panels tested, figure 10, in this study. Once the diagonal tension field is established in the panel, the panel strength is a function of the material strength parallel to the tension field (buckles). Forces normal to the buckles are small relative to the forces parallel to the tension field. Typical failure modes of thin shear panels were tension failures perpendicular to the buckle direction.

When impact conditions affect component design requirements, the designer needs simplified charts, tables, or analytical procedures to predict performance. One such analytical procedure is the point stress failure criterion. The point stress failure criterion has been shown to correlate well with failures of composite panels with holes and cracks (ref. 12).

The point stress failure criterion assumes that failure occurs when the stresses at a small distance, D_0, away from the edge of a discontinuity reach the material strength. This criterion is a two-parameter criterion with parameters D_0 and material strength determined empirically. A D_0 value of approximately 0.13 cm (0.05 in.) is considered typical.

The point stress failure criterion (ref. 9) for an infinite orthotropic plate with a hole of radius a, as depicted in figure 11, is given by

$$\frac{\sigma_N^\infty}{\sigma_0} = \frac{2}{2 + \xi^2 + 3\xi^4 - (K_t - 3)(5\xi^6 - 7\xi^8)} \qquad (1)$$

where

$$K_t = 1 + \sqrt{2\left(\sqrt{\frac{E_y}{E_x}} - \nu_{xy}\right) + \frac{E_y}{G_{xy}}}$$

and $\xi = a/(a + D_0)$. The applied far-field stress and the stress at $x = a + D_0$, $y = 0$ are σ_N^∞ and σ_0, respectively. The longitudinal and transverse extensional moduli, shear modulus, and Poisson's ratio are E_x, E_y, G_{xy}, ν_{xy}, respectively. Similarly, the point stress criterion for an infinite orthotropic plate with a crack of half length a (see fig. 11) is given

by

$$\frac{\sigma_N^{\infty}}{\sigma_0} = \sqrt{1 - \xi^2} \qquad (2)$$

where $\xi = a/(a + D_0)$.

Predicted values from equations (1) and (2) were compared with the low-velocity and ballistic impact tests of the composite panels, respectively. For the nonpenetrating impacts, the hole radius was taken as half the distance across the visually detected damaged region. Hole radius, a, for the penetrating low-velocity impacts includes the penetration and any delamination damage around the penetration. (See fig. 12.) The crack length, $2a$, for the ballistic impact tests was taken as the length of the damaged region perpendicular to the diagonal tension field (buckles). (See fig. 12.)

Discussion of Results

Undamaged Panels

Shear strength tests on undamaged composite and aluminum panels were conducted as previously described. Ultimate shear stress resultants for each panel are listed in table V and plotted in figure 13. The ultimate shear stress resultant is calculated by dividing the applied edge failure load by the length of the panel. The average ultimate shear stress resultants for panels with all three aspect ratios for each of the four material configurations were calculated and compared with values obtained for damaged panels. Average ultimate shear stress resultants for panels with a particular aspect ratio varied less than 15 percent from values obtained for panels of the same material with other aspect ratios. There are no distinguishable trends with respect to panel ultimate shear stress resultant and aspect ratio. All panels except the $[+30^F/-60^F]_s$ K/E panels exhibited tension failures across a buckle similar to those reported in reference 10. The $[+30^F/-60^F]_s$ K/E panels exhibited a combined tension and shear failure. The combined failure mode of the $[+30^F/-60^F]_s$ K/E is attributed to the nonalignment of fibers with the diagonal tension forces.

Panels Damaged by Low-Velocity Impact

The low-velocity impact tests consisted of impacting 23 composite panels at 46 m/sec (150 ft/sec) and 22 composite panels at 67 m/sec (220 ft/sec) with a 1.27-cm (0.50-in.) diameter aluminum sphere. The impacts at 46 m/sec (150 ft/sec) did not penetrate the panels, whereas the impacts at 67 m/sec (220 ft/sec) penetrated the panels. The residual strengths of the low-velocity nonpenetrating and penetrating impact tests are listed in table VI. The residual strength ratio (i.e., the strength of the damaged panel divided by the average strength of the undamaged panels) is plotted in figure 14.

Typical strength reduction as a result of the nonpenetrating impact was negligible. Strength reductions were typically within the data scatter of the tests on undamaged panels. The visible damaged area on the impact side of the composite panels was a circular region less than 0.64 cm (0.25 in.) across, as shown in figure 15. Little or no visible back side damage was observed. All panels had failure modes similar to those of the undamaged panels. The failure did not necessarily coincide with the impact point.

Typical strength reductions from penetrating impacts were 15 to 20 percent of the undamaged-panel strength. Visual and C-scan-defined damage areas were comparable. As shown in figures 16 and 17, typical entrance and exit side damage was between 1.27 cm (0.50 in.) and 1.91 cm (0.75 in.) across for both K/E and K-Gr/E panels. Exit side damage consisted of frayed Kevlar fibers about the penetration with delamination around the perimeter of the penetration. Entrance side damage consisted of the hole with little or no perimeter delamination. The Gr/E plies in the hybrid laminates were cleanly penetrated by the aluminum sphere. All panels were tested to measure residual strength. They exhibited the characteristic tension failure with failure initiating at the hole and propagating to the edge of the panel. (See fig. 18.)

Panels Damaged by Ballistic Impact

Composite and aluminum shear panels were ballistically impacted while subjected to a shear load. Panel failure when impacted was defined as a tension failure perpendicular to the buckle extending across the test section of the panel. Typical panel failure modes of panels not surviving impact are shown in figures 19 and 20. Panels that did not exhibit the diagonal tension failure mode were considered to have survived the impact regardless of the extent of damage.

The threshold load for panels of a particular material configuration and panel aspect ratio, as previously stated in this study, is defined by the panel that has the lowest average load of the preimpact load and the residual load. For the purpose of computing the threshold load, if a panel survives the impact (as determined by the previous definition of panel failure) but has a residual strength of less than the applied load when impacted, then it is assumed to have failed upon impact. Furthermore, if panels of the same aspect ratio and material have the same load at impact and one or more panels fail whereas

the others survive impact, then the threshold load is assumed to be the applied load at impact.

Precise control of the projectile tumble and orientation angles was not achievable. Tables VII–IX list the projectile tumble and orientation angles for the ballistically impacted panel tests. The projectile tumble angle (α), as shown in figure 21, is the enclosed angle between the longitudinal axis of the projectile and the normal axis (through the thickness) of the panel. Projectile orientation angle (θ), see figure 21, is the angle between the longitudinal axis of the projectile and the inplane horizontal axis of the panel. Figure 22 shows the effect of tumble angle on the crack length ($2a$). As the crack length ($2a$) approaches the diameter of the projectile, the projectile tumble angle approaches zero. Figure 23 shows the effect of projectile orientation angle on the crack length ($2a$). The smallest crack length ($2a$) occurs for orientation angles between 30° and 65°; this is consistent with the definition of the crack length ($2a$). Data scatter and the coupling effects between projectile tumble angle and orientation angle hinder the discerning of other characteristics. The results of the low-velocity and ballistic impact tests suggest that nontumbled ballistic impacts ($\alpha = 0°$) would cause no greater damage than an equivalent diameter spherical projectile that penetrated the panel at a lower speed.

Figure 24 presents data on the effect of crack length ($2a$) on residual panel strength. As the crack length ($2a$) decreases, the residual strength increases. When the crack length approaches the diameter of the projectile, the residual strength is approximately equal to the residual strength of those panels that were subjected to penetrating low-velocity impacts.

Aluminum panels. When the aluminum panels were ballistically impacted, a bright flash occurred at impact. The flash corresponded to burning aluminum as the projectile penetrated the panel. At the edge of the hole, the panel skin tore and formed numerous cracks. Typical ballistic damage of aluminum panels is shown in figure 25. By the previously described definition of panel failure, no aluminum panel failed. This was primarily a result of the constant displacement load train.

The load applied before impact to the panels varied between 54 and 94 percent of the undamaged-panel strength. The residual panel load was lower than the applied load when impacted for 8 of the 10 aluminum panels tested. These results are plotted in figure 26. The criterion used to estimate the threshold load for the aluminum panels with an aspect ratio of 1.000 was modified from that previously stated because the residual loads of all aluminum panels were less than the applied loads when impacted. The threshold load was estimated to be the average of the applied load when impacted and the average residual load for the three panels tested. The threshold load ratios, plotted in figure 26 and listed in table X, were 0.65, 0.59, and 0.59 for the aluminum panels with aspect ratios of 1.000, 1.625, and 2.500, respectively. Average threshold load ratio for aluminum panels with all three aspect ratios was 0.61 of the failure load of the undamaged aluminum panels.

The residual strengths of ballistically impacted aluminum shear panels are plotted in figure 26. The average residual strengths, listed in table XI, were 0.45, 0.60, and 0.67 of the strength of the undamaged aluminum panels for panels having aspect ratios of 1.000, 1.625, and 2.500, respectively, with an overall average of 0.57. The average residual strengths increased with panel aspect ratio. The average crack lengths of panels having different aspect ratios were similar, and the extent of damage was similar. Therefore, the percent of damaged area of the panel should decrease with increased aspect ratio, and the residual strength should increase.

Composite panels. For tumble angles less than 30°, the ballistically impacted composite panels exhibited similar damage to that of the penetrated low-velocity-impacted panels. The front side of the panel had frayed Kevlar fibers with some delamination around the perimeter of the penetration. Figure 27 shows typical damage for a ballistically impacted K/E panel with a tumble angle of 20°. The exit side showed slightly more delamination and fraying of Kevlar fibers than the impacted side. The damage area on the exit side of the K-Gr/E hybrid panels was greater than on the K/E panels. The outer Kevlar ply of the hybrid panels had a larger delaminated area around the penetration, as shown in figure 28, than the K/E panels. The graphite inner plies of the K-Gr/E hybrid panels were penetrated by the projectile with no distinguishable edge delamination.

As the tumble angle increases, the impact and exit side damage increases. The impact side damage for both K/E panels and K-Gr/E panels consists of the penetration and some perimeter delamination. The exit side damage was more extensive. Typically, the outer two plies on the exit side of the K/E panels delaminate around the penetration site, as shown in figure 29. Figure 30 shows that extensive delamination of the outer Kevlar ply on the exit side occurs for the K-Gr/E panels. The graphite inner plies were penetrated with no distinguishable delamination around the perimeter. Those panels

that failed when impacted did not exhibit any other damage characteristics around the penetration than those previously described.

Figures 31–33 present data on the applied load ratio when impacted, the residual ultimate load ratio, and the threshold load ratios for ballistically impacted panels. The threshold load was calculated as initially described. The average threshold loads for the composite panels are presented in table X. The average threshold loads ratio for the $[\pm 45^F]_s$ K/E, $[+45^F_K/-45^F_{Gr}]_s$ K-Gr/E, and $[+30^F/-60^F]_s$ K/E panels were 0.44, 0.48, and 0.55 of the average undamaged-panel strength, respectively. No consistent trends were identified with respect to threshold load and panel aspect ratio for the composite panels. The threshold load for the $[\pm 45^F]_s$ K/E panels with an aspect ratio of 1.000 was inconsistent with the other threshold load results. The first specimen for this configuration and aspect ratio was ballistically impacted while loaded to 0.66 of the average undamaged-panel failure load. The specimen did not fail when impacted. Based upon previous tests, this load was sufficient to cause failure of the panel upon impact. The tumble angle and crack length ($2a$) were small, so the impact had less effect on residual strength than expected. The second specimen was loaded to 79 percent of the average undamaged-panel strength. When impacted, the panel failed. The first specimen was assumed to be typical, and the first test conditions were repeated for the third specimen. The crack length of the third specimen was more than three times that produced in the first specimen. The third specimen failed upon impact. Because it was not known whether the first or third specimen was typical, the first conditions were reapplied to the fourth specimen. The specimen failed upon impact. The crack length was twice that of the first specimen. In hindsight, the fourth specimen should have been loaded to 45 or 50 percent of the average undamaged-panel strength. Hence the threshold load data are suspect for the $[\pm 45^F]_s$ K/E panel having an aspect ratio of 1.000.

The average panel residual strength ratios are presented in table XI. The average panel residual strength ratios for $[\pm 45^F]_s$ K/E, $[+45^F_K/-45^F_{Gr}]_s$ K-Gr/E, and $[+30^F/-60^F]_s$ K/E panels were 0.55, 0.55, and 0.75 of the average undamaged-panel strength, respectively. No trends were identified with respect to threshold load and panel aspect ratio.

Correlation of Analytical and Experimental Results

The point stress failure criteria as represented by equations (1) and (2) were used to compare the predicted values with the low-velocity and ballistically impacted composite panel test results. As previously discussed, the postbuckling response of the thin composite panels tested in this study is primarily a function of the mechanical material properties parallel to the tension field. The stress ratio σ_N^∞/σ_0 from equation (1) and test data from the low-velocity-impacted panels were plotted versus the crack length ($2a$) in figures 34–36 for the $[\pm 45^F]_s$ K/E, $[+45^F_K/-45^F_{Gr}]_s$ K-Gr/E, and $[+30^F/-60^F]_s$ K/E panels. Tensile stress at failure, σ_N^∞, parallel to the tension field was computed by the equation

$$\sigma_N^\infty = \frac{2N_{xy}}{t}$$

from reference 11, where t is panel thickness and N_{xy} is the applied edge shear stress resultant when the panel failed. The undamaged material strength, σ_0, was determined from coupon tests. As shown in figures 34–36, typical values of D_0 that correlate with the test data were between 0.05 cm (0.02 in.) and 0.20 cm (0.08 in.). These results are in agreement with the results from tension tests in reference 12.

The point stress criterion for a crack, equation (2), was used to compare the predicted values with data obtained for the ballistically impacted composite panels. Test data analogous to those for the low-velocity-impacted panels were prepared. The stress ratio from equation (2) and the test results for the $[\pm 45^F]_s$ K/E, $[+45^F_K/-45^F_{Gr}]_s$ K-Gr/E, and $[+30^F/-60^F]_s$ K/E panels are plotted in figures 37–39. The test results correlated with point stress criteria with values of D_0 from 0.03 cm (0.01 in.) to 0.20 cm (0.08 in.).

Concluding Remarks

The effects of low-velocity and ballistic impact damage on thin composite and aluminum shear panels were determined. All ballistically impacted panels were loaded and impacted with a tumbled 0.50-caliber projectile. The following remarks are based on results of this study.

Panel aspect ratio was not found to be a significant characteristic parameter of panel strength. The $[\pm 45^F]_s$ Kevlar/epoxy (K/E) and $[+45^F_K/-45^F_{Gr}]_s$ Kevlar-graphite/epoxy (K-Gr/E) panels exhibited tension failures perpendicular to the tension field. The $[+30^F/-60^F]_s$ K/E panels had a combined tension and shear failure attributed to nonalignment of fibers with the diagonal tension forces.

Typically, strength reduction from nonpenetrating low-velocity impacts was negligible. The typical damaged area of the nonpenetrated low-velocity-impacted panels was a circular region less than

0.64 cm (0.25 in.) across on the impacted side with little or no visible damage on the back side. A 15- to 20-percent reduction in residual strength from the undamaged-panel strength was typically obtained from the penetrating low-velocity impact tests. The damaged region of the penetrated low-velocity-impacted panels consisted of delamination around the perimeter of the penetration. The damage was approximately 1.91 cm (0.75 in.) across.

The results of the low-velocity and ballistic impact tests suggest that nontumbled ballistic impacts (projectile tumble angle of 0°) would cause no greater damage than an equivalent diameter spherical projectile that penetrated the panel at a lower speed.

The average threshold load for all ballistically impacted aluminum panels was 0.61 of the average failure load for the undamaged aluminum panels. Average residual strength for aluminum panels was 0.57 of the average undamaged-aluminum-panel strength.

The average threshold loads for ballistically impacted $[\pm 45^{F}]_s$ K/E, $[+45^{F}_{K}/-45^{F}_{Gr}]_s$ K-Gr/E, and $[+30^{F}/-60^{F}]_s$ K/E panels were 0.44, 0.48, and 0.55, respectively, of the average undamaged-panel failure load. The average panel residual strengths were 0.55, 0.55, and 0.75 of the average undamaged-panel strength for the $[\pm 45^{F}]_s$ K/E, $[+45^{F}_{K}/-45^{F}_{Gr}]_s$ K-Gr/E, and $[+30^{F}/-60^{F}]_s$ K/E panels, respectively. Exit side damage of the panels consisted of extensive delamination of the outer ply around the penetration. The entrance side exhibited outer ply delamination about the perimeter of the penetration, though not as extensive as on the exit side.

The point stress failure criteria for a hole and a crack in infinite panels correlated well with the low-velocity and ballistic impact test results, respectively.

NASA Langley Research Center
Hampton, VA 23665
February 19, 1985

References

1. Slepetz, John M.; Oplinger, Donald W.; Parker, Burton S.; and Tremblay, Robert T.: *Impact Damage Tolerance of Graphite/Epoxy Sandwich Panels.* AMMRC TR 74-20, U.S. Army, Sept. 1974.
2. Rhodes, Marvin D.: *Impact Tests on Fibrous Composite Sandwich Structure.* NASA TM-78719, 1978.
3. Williams, Jerry G.; and Rhodes, Marvin D.: *The Effect of Resin on the Impact Damage Tolerance of Graphite-Epoxy Laminates.* NASA TM-83213, 1981.
4. Rhodes, Marvin D.; Williams, Jerry G.; and Starnes, James H., Jr.: *Effect of Low Velocity Impact Damage on the Compressive Strength of Graphite/Epoxy Hat-Stiffened Panels.* NASA TM X-73988, 1976.
5. Rhodes, Marvin D.; and Williams, Jerry G.: Concepts for Improving the Damage Tolerance of Composite Compression Panels. NASA paper presented at 5th DOD/NASA Conference on Fibrous Composites in Structural Design (New Orleans, LA) Jan. 27–29, 1981.
6. Olster, E. F.; and Roy, P. A.: Tolerance of Advanced Composites to Ballistic Damage. *Composite Materials: Testing and Design (Third Conference),* ASTM Spec. Tech. Publ. 546, 1974, pp. 583–603.
7. Avery, J. G.; and Porter, T. R.: Comparisons of the Ballistic Impact Response of Metals and Composites for Military Aircraft Applications. *Foreign Object Impact Damage to Composites,* ASTM Spec. Tech. Publ. 568, c.1975, pp. 3–29.
8. Mayerjak, Robert J.; and Singley, George T., III: Composite Rotor Hub. Preprint No. 77.33.82, 33rd Annual National Forum, American Helicopter Soc., Inc., May 1977.
9. Whitney, James M.: Notch Strength of Composites. *Failure Analysis and Mechanisms of Failure of Fibrous Composite Structures,* Ahmed K. Noor, Mark J. Shuart, James H. Starnes, Jr., and Jerry G. Williams, compilers, NASA CP-2278, 1983, pp. 241–263.
10. Farley, Gary L.; and Baker, Donald J.: In-Plane Shear Test of Thin Panels. *Exper. Mech.,* vol. 23, no. 1, Mar. 1983, pp. 81–88.
11. Kuhn, Paul; Peterson, James P.; and Levin, L. Ross: *A Summary of Diagonal Tension. Part I—Methods of Analysis.* NACA TN 2661, 1952.
12. Whitney, J. M.; and Nuismer, R. J.: Stress Fracture Criteria for Laminated Composites Containing Stress Concentrations. *J. Compos. Mater.,* vol. 8, July 1974, pp. 253–265.

TABLE I. LOW-VELOCITY IMPACT TEST CONDITIONS

[Projectile was Al sphere with diameter of 1.27 cm (0.50 in.)]

Panel description and specimen number (a)	Speed of projectile, m/sec (ft/sec), impacting shear panel with aspect ratio[b] of—		
	1.000 (c)	1.625 (c)	2.500 (c)
$[\pm 45^{F}]_s$ K/E			
1	47 (155)	47 (154)	48 (156)
2	47 (154)	68 (224)^P	65 (214)^P
3	69 (227)^P		
4	68 (222)^P		
$[+45^{F}_{K}/-45^{F}_{Gr}]_s$ K-Gr/E			
1	47 (154)	45 (149)	46 (150)
2	47 (154)	46 (151)	45 (149)
3	68 (224)^P	67 (220)^P	67 (221)^P
4	66 (217)^P	67 (221)^P	66 (217)^P
$[+30^{F}/-60^{F}]_s$ K/E			
1	45 (149)		47 (154)
2	46 (151)		69 (228)^P
3	67 (219)^P		
4	68 (222)^P		

[a] E Narmco 5208 epoxy resin
F fabric
Gr Thornel 300 graphite fiber
K Kevlar 49 fiber
s symmetric

[b] Panel aspect ratio — Panel dimensions, cm (in.)
1.000 — 20.3 × 20.3 (8.0 × 8.0)
1.625 — 20.3 × 33.0 (8.0 × 13.0)
2.500 — 20.3 × 50.8 (8.0 × 20.0)

[c] P indicates that projectile penetrated panel.

TABLE II. BALLISTIC IMPACT TEST CONDITIONS OF SHEAR PANELS WITH ASPECT RATIO OF 1.000

[All panels had test-section dimensions of 20.3 cm × 20.3 cm (8.0 in. × 8.0 in.)]

Panel description and specimen number (a)	Applied stress resultant		Impact speed, m/sec (ft/sec)
	N_{xy}, kN/m (lbf/in.)	Percent of static ultimate	
6061-T6 aluminum			
1	140.1 (800)	82.9	682.8 (2240)
2	140.1 (800)	82.9	695.6 (2282)
3	140.1 (800)	82.9	677.6 (2223)
$[\pm 45^{F}]_{s}$ K/E			
1	65.7 (375)	66.3	686.7 (2253)
2	78.8 (450)	79.5	681.5 (2236)
3	65.7 (375)	66.3	673.9 (2211)
4	65.7 (375)	66.3	683.4 (2242)
$[+45^{F}_{K}/-45^{F}_{Gr}]_{s}$ K-Gr/E			
1	65.7 (375)	49.5	691.9 (2270)
2	87.6 (500)	65.9	680.3 (2232)
3	65.7 (375)	49.5	692.5 (2272)
4	65.7 (375)	49.5	683.9 (2244)
$[+30^{F}/-60^{F}]_{s}$ K/E			
1	65.7 (375)	69.4	676.0 (2218)
2	46.0 (263)	48.7	679.1 (2228)
3	46.0 (263)	48.7	685.8 (2250)
4	46.0 (263)	48.7	681.5 (2236)

[a] E Narmco 5208 epoxy resin
F fabric
Gr Thornel 300 graphite fiber
K Kevlar 49 fiber
s symmetric

TABLE III. BALLISTIC IMPACT TEST CONDITIONS OF SHEAR PANELS WITH ASPECT RATIO OF 1.625

[All panels had test-section dimensions of 20.3 cm × 33.0 cm (8.0 in. × 13.0 in.)]

Panel description and specimen number (a)	Applied stress resultant		Impact speed, m/sec (ft/sec)
	N_{xy}, kN/m (lbf/in.)	Percent of static ultimate	
6061-T6 aluminum			
1	83.5 (477)	54.0	682.8 (2240)
2	122.6 (700)	79.3	693.4 (2275)
3	137.5 (785)	88.9	676.9 (2221)
$[\pm 45^{F}]_{s}$ K/E			
1	66.0 (377)	68.8	697.9 (2290)
2	44.5 (254)	46.4	687.3 (2255)
3	44.5 (254)	46.4	689.8 (2263)
4	44.5 (254)	46.4	687.0 (2254)
$[+45^{F}_{K}/-45^{F}_{Gr}]_{s}$ K-Gr/E			
1	63.4 (362)	51.6	664.8 (2181)
2	74.1 (423)	60.3	681.8 (2237)
3	63.4 (362)	51.6	703.8 (2309)
4	63.4 (362)	51.6	680.3 (2232)
$[+30^{F}/-60^{F}]_{s}$ K/E			
1	53.9 (308)	63.5	681.8 (2237)
2	48.5 (277)	57.1	678.2 (2225)
3	48.5 (277)	57.1	687.6 (2256)

[a] E Narmco 5208 epoxy resin
F fabric
Gr Thornel 300 graphite fiber
K Kevlar 49 fiber
s symmetric

TABLE IV. BALLISTIC IMPACT TEST CONDITIONS OF SHEAR PANELS WITH ASPECT RATIO OF 2.500

[All panels had test-section dimensions of 20.3 cm × 50.8 cm (8.0 in. × 20.0 in.)]

Panel description and specimen number (a)	Applied stress resultant		Impact speed, m/sec (ft/sec)
	N_{xy}, kN/m (lbf/in.)	Percent of static ultimate	
6061-T6 aluminum			
1	83.2 (475)	55.7	697.1 (2287)
2	122.6 (700)	82.1	686.1 (2251)
3	140.1 (800)	93.8	691.6 (2269)
$[\pm 45^{F}]_{s}$ K/E			
1	65.7 (375)	57.9	684.3 (2245)
2	32.9 (188)	29.0	674.2 (2212)
3	46.1 (263)	40.6	680.9 (2234)
4	46.1 (263)	40.6	687.3 (2255)
5	46.1 (263)	40.6	693.7 (2276)
$[+45^{F}_{K}/-45^{F}_{Gr}]_{s}$ K-Gr/E			
1	65.7 (375)	48.3	680.0 (2231)
2	32.9 (188)	24.2	675.4 (2216)
3	46.1 (263)	33.8	686.4 (2252)
4	46.1 (263)	33.8	684.3 (2245)
5	46.1 (263)	33.8	681.2 (2235)
$[+30^{F}/-60^{F}]_{s}$ K/E			
1	48.2 (275)	50.8	640.4 (2101)
2	48.2 (275)	50.8	689.8 (2263)
3	65.7 (375)	69.3	688.2 (2258)
4	56.0 (320)	59.1	665.7 (2184)
5	48.2 (275)	50.8	683.4 (2242)

[a] E Narmco 5208 epoxy resin
F fabric
Gr Thornel 300 graphite fiber
K Kevlar 49 fiber
s symmetric

TABLE V. ULTIMATE SHEAR STRESS RESULTANT OF UNDAMAGED PANELS

Panel description (a)	Ultimate shear stress resultant, N_{xy}, kN/m (lbf/in.), for panel with aspect ratio[b] of—					
	1.000		1.625		2.500	
6061-T6 aluminum	166	(950)	153	(873)	159	(910)
	171	(975)	182	(1038)	139	(795)
	169	(968)	129	(738)	149	(852)
	-----	------	155	(883)	-----	------
Average	169	(964)	155	(883)	149	(852)
$[\pm 45^{F}]_s$ K/E	103	(588)	97	(554)	114	(650)
	97	(556)	96	(550)	116	(665)
	97	(554)	95	(542)	110	(626)
Average	99	(566)	96	(548)	113	(647)
$[\pm 45^{F}_{K}/-45^{F}_{Gr}]_s$ K-Gr/E	128	(731)	105	(600)	145	(828)
	136	(775)	145	(827)	129	(735)
	134	(768)	118	(677)	134	(765)
Average	133	(758)	123	(701)	136	(776)
$[+30^{F}/-60^{F}]_s$ K/E	105	(600)	85	(485)	81	(463)
	78	(444)	85	(485)	107	(613)
	101	(577)	85	(485)	96	(548)
Average	95	(540)	85	(485)	95	(541)

[a]E Narmco 5208 epoxy resin
F fabric
Gr Thornel 300 graphite fiber
K Kevlar 49 fiber
s symmetric

[b]Panel aspect ratio — Panel dimensions, cm (in.)
1.000 — 20.3 × 20.3 (8.0 × 8.0)
1.625 — 20.3 × 33.0 (8.0 × 13.0)
2.500 — 20.3 × 50.8 (8.0 × 20.0)

TABLE VI. ULTIMATE RESIDUAL SHEAR STRESS RESULTANT OF PANELS IMPACTED AT LOW VELOCITY

Panel description and specimen number (a)	Ultimate shear stress resultant for panel with aspect ratio of—					
	1.000 (c)		1.625 (c)		2.500 (c)	
	N_{xy}, kN/m (lbf/in.)	Percent of undamaged	N_{xy}, kN/m (lbf/in.)	Percent of undamaged	N_{xy}, kN/m (lbf/in.)	Percent of undamaged
$[\pm 45^{F}]_s$ K/E						
1	92 (528)	93.2	94 (538)	98.1	111 (637)	98.5
2	94 (534)	94.3	81 (464)	84.7^{P}	88 (503)	77.7^{P}
3	79 (451)	79.7^{P}				
4	84 (478)	84.4^{P}				
$[+45^{F}_{K}/-45^{F}_{Gr}]_s$ K-Gr/E						
1	136 (778)	102.5	110 (627)	89.5	138 (791)	101.9
2	136 (775)	102.2	139 (795)	113.4	123 (702)	90.5
3	106 (608)	80.1^{P}	105 (598)	85.4^{P}	110 (626)	80.7^{P}
4	110 (631)	83.3^{P}	101 (577)	82.3^{P}	108 (619)	79.8^{P}
$[+30^{F}/-60^{F}]_s$ K/E						
1	102 (584)	108.1			97 (555)	102.5
2	102 (584)	108.1			100 (569)	105.1^{P}
3	98 (558)	103.3^{P}				
4	79 (450)	83.3^{P}				

[a] E Narmco 5208 epoxy resin
F fabric
Gr Thornel 300 graphite fiber
K Kevlar 49 fiber
s symmetric

[b] Panel aspect ratio — Panel dimensions, cm (in.)
1.000 — 20.3 × 20.3 (8.0 × 8.0)
1.625 — 20.3 × 33.0 (8.0 × 13.0)
2.500 — 20.3 × 50.8 (8.0 × 20.0)

[c] P indicates that projectile penetrated panel.

TABLE VII. TEST RESULTS OF BALLISTICALLY IMPACTED SHEAR PANELS WITH ASPECT RATIO OF 1.000

[All panels had test-section dimensions of 20.3 cm × 20.3 cm (8.0 in. × 8.0 in.)]

Panel description and specimen number (a)	Panel failed when impacted?	Projectile			Crack length, $2a$, cm (in.)	Ultimate residual shear stress resultant	
		Tumble angle, deg	Projected length, cm (in.)	Orientation angle, deg		N_{xy}, kN/m (lbf/in.)	Percent of undamaged
6061-T6 aluminum							
1	No	90	6.04 (2.38)	86	4.6 (1.8)	64.6 (369)	38.3
2	No	90	6.04 (2.38)	87	5.1 (2.0)	76.2 (435)	45.1
3	No	59	4.93 (1.94)	−172	4.3 (1.7)	88.4 (505)	52.4
$[\pm 45^{F}]_{s}$ K/E							
1	No	69	5.41 (2.13)	37	2.3 (0.9)	77.6 (443)	78.3
2	Yes	80	5.72 (2.25)	17	4.1 (1.6)		
3	Yes	71	5.56 (2.19)	95	7.9 (3.1)		
4	Yes	80	5.72 (2.25)	86	5.1 (2.0)		
$[+45^{F}_{K}/-45^{F}_{Gr}]_{s}$ K-Gr/E							
1	No	56	4.78 (1.88)	160	4.3 (1.7)	73.2 (418)	55.1
2	Yes	80	5.72 (2.25)	105	5.3 (2.1)		
3	No	56	4.78 (1.88)	130	5.3 (2.1)	65.8 (376)	49.6
4	No	71	5.56 (2.19)	99	4.8 (1.9)	70.2 (401)	52.9
$[+30^{F}/-60^{F}]_{s}$ K/E							
1	Yes	56	4.78 (1.88)	−118	2.0 (0.8)		
2	No	80	5.72 (2.25)	90	4.3 (1.7)	68.3 (390)	72.2
3	No	27	2.54 (1.00)	100	2.8 (1.1)	76.4 (436)	80.7
4	No	71	5.56 (2.19)	60	3.6 (1.4)	49.6 (283)	52.4

[a] E Narmco 5208 epoxy resin
F fabric
Gr Thornel 300 graphite fiber
K Kevlar 49 fiber
s symmetric

TABLE VIII. TEST RESULTS OF BALLISTICALLY IMPACTED SHEAR PANELS WITH ASPECT RATIO OF 1.625

[All panels had test-section dimensions of 20.3 cm × 33.0 cm (8.0 in. × 13.0 in.)]

Panel description and specimen number (a)	Panel failed when impacted?	Projectile			Crack length, $2a$, cm (in.)	Ultimate residual shear stress resultant	
		Tumble angle, deg	Projected length, cm (in.)	Orientation angle, deg		N_{xy}, kN/m (lbf/in.)	Percent of undamaged
6061-T6 aluminum							
1	No	45	4.14 (1.63)	145	4.6 (1.8)	94.6 (540)	61.2
2	No	80	5.72 (2.25)	74	3.8 (1.5)	102.1 (583)	66.0
3	No	90	6.05 (2.38)	85	4.8 (1.9)	79.5 (454)	51.4
$[\pm 45^{F}]_{s}$ K/E							
1	Yes	54	4.59 (1.81)	−25	4.6 (1.8)		
2	No	71	5.56 (2.19)	105	5.8 (2.3)	66.5 (380)	69.3
3	No	80	5.72 (2.25)	70	4.3 (1.7)	31.1 (178)	32.5
4	No	40	3.81 (1.50)	−153	2.3 (0.9)	62.5 (357)	65.1
$[+45^{F}_{K}/-45^{F}_{Gr}]_{s}$ K-Gr/E							
1	No	80	5.72 (2.25)	101	5.1 (2.0)	66.0 (377)	53.7
2	Yes	45	4.14 (1.63)	70	2.3 (0.9)		
3	No	80	5.72 (2.25)	−55	5.8 (2.3)	41.7 (238)	33.9
4	No	49	4.29 (1.69)	115	4.6 (1.8)	67.9 (388)	55.3
$[+30^{F}/-60^{F}]_{s}$ K/E							
1	Yes	71	5.56 (2.19)	73	2.8 (1.1)		
2	No	71	5.56 (2.19)	122	5.6 (2.2)	57.9 (331)	68.2
3	No	56	4.78 (1.88)	−109	2.0 (0.8)	72.2 (412)	84.9

[a] E Narmco 5208 epoxy resin
F fabric
Gr Thornel 300 graphite fiber
K Kevlar 49 fiber
s symmetric

TABLE IX. TEST RESULTS OF BALLISTICALLY IMPACTED SHEAR PANELS WITH ASPECT RATIO OF 2.500

[All panels had test-section dimensions of 20.3 cm × 50.8 cm (8.0 in. × 20.0 in.)]

Panel description and specimen number (a)	Panel failed when impacted?	Projectile			Crack length, $2a$, cm (in.)	Ultimate residual shear stress resultant	
		Tumble angle, deg	Projected length, cm (in.)	Orientation angle, deg		N_{xy}, kN/m (lbf/in.)	Percent of undamaged
6061-T6 aluminum							
1	No	68	5.23 (2.06)	97	4.6 (1.8)	90.4 (516)	60.6
2	No	90	6.04 (2.38)	83	4.6 (1.8)	96.3 (550)	64.6
3	No	90	6.04 (2.38)	−130	3.6 (1.4)	111.0 (634)	74.4
$[\pm 45^{F}]_s$ K/E							
1	Yes	71	5.56 (2.19)	145	5.6 (2.2)		
2	No	16	1.75 (0.69)	25	1.8 (0.7)	90.9 (519)	80.2
3	No	50	4.44 (1.75)	35	2.3 (0.9)	73.0 (417)	64.5
4	No	80	5.71 (2.25)	100	4.6 (1.8)	30.3 (173)	26.7
5	No	80	5.71 (2.25)	95	4.6 (1.8)	43.8 (250)	38.6
$[+45^{F}_{K}/-45^{F}_{Gr}]_s$ K-Gr/E							
1	Yes	69	5.41 (2.13)	121	5.8 (2.3)		
2	No	45	4.14 (1.63)	108	4.1 (1.6)	69.4 (396)	51.0
3	No	90	6.04 (2.38)	−156	3.0 (1.2)	64.9 (371)	47.8
4	No	29	2.87 (1.13)	60	2.0 (0.8)	112.6 (643)	82.9
5	No	50	4.44 (1.75)	55	1.8 (0.7)	104.0 (594)	76.5
$[+30^{F}/-60^{F}]_s$ K/E							
1	No	24	2.38 (0.94)	65	1.5 (0.6)	84.6 (483)	89.3
2	No	69	5.41 (2.13)	73	3.0 (1.2)	65.8 (376)	69.5
3	Yes	90	6.04 (2.38)	142	5.8 (2.3)		
4	Yes	90	6.04 (2.38)	142	6.4 (2.5)		
5	Yes	60	5.08 (2.00)	94	3.3 (1.3)		

[a] E Narmco 5208 epoxy resin
F fabric
Gr Thornel 300 graphite fiber
K Kevlar 49 fiber
s symmetric

TABLE X. THRESHOLD LOAD RATIO OF ALUMINUM AND COMPOSITE BALLISTICALLY DAMAGED SHEAR PANELS

Panel description (a)	Threshold load / Average failure load of undamaged panels			
	Panel with aspect ratio of—			
	1.000	1.625	2.500	Average
6061-T6 aluminum	0.65	0.59	0.59	0.61
$[\pm 45^{F}]_s$ K/E	[b]0.66	0.46	0.41	[c]0.44
$[+45^{F}_{K}/-45^{F}_{Gr}]_s$ K-Gr/E	0.50	0.52	0.41	0.48
$[+30^{F}/-60^{F}]_s$ K/E	0.52	0.62	0.51	0.55

[a]E Narmco 5208 epoxy resin
F fabric
Gr Thornel 300 graphite fiber
K Kevlar 49 fiber
s symmetric
[b]Data are suspect.
[c]Does not include suspect data.

TABLE XI. AVERAGE PANEL RESIDUAL STRENGTH RATIO OF ALUMINUM AND COMPOSITE BALLISTICALLY DAMAGED PANELS

Panel description (a)	Average panel residual strength / Average undamaged panel strength			
	Panel with aspect ratio of—			
	1.000	1.625	2.500	Average
6061-T6 aluminum	0.45	0.60	0.67	0.57
$[\pm 45^{F}]_s$ K/E	[b]0.78	0.56	0.53	[c]0.55
$[+45^{F}_{K}/-45^{F}_{Gr}]_s$ K-Gr/E	0.53	0.48	0.65	0.55
$[+30^{F}/-60^{F}]_s$ K/E	0.68	0.77	0.79	0.75

[a]E Narmco 5208 epoxy resin
F fabric
Gr Thornel 300 graphite fiber
K Kevlar 49 fiber
s symmetric
[b]One specimen.
[c]Data for panel with aspect ratio of 1.000 were excluded.

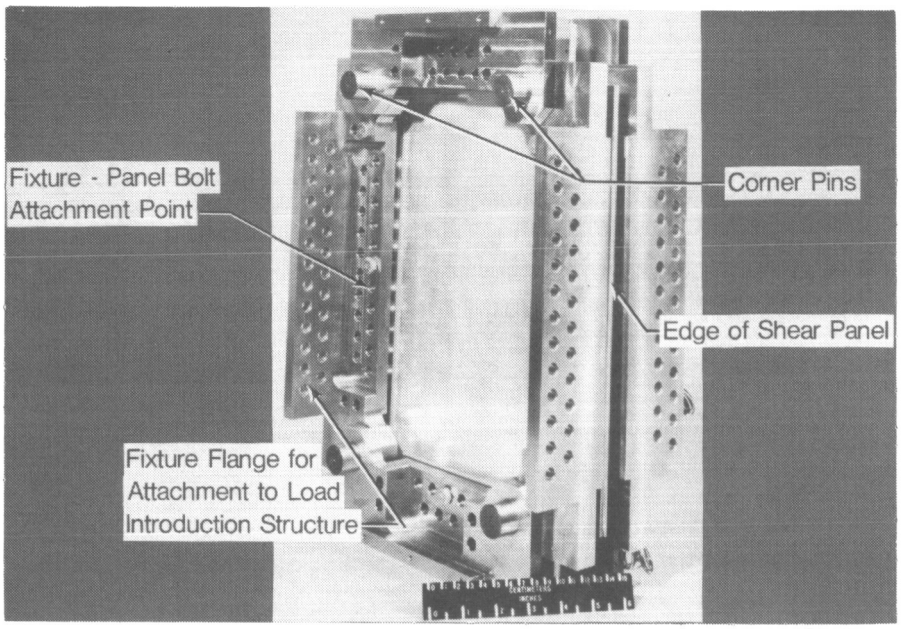

L-85-29

Figure 1. Improved picture frame shear fixture.

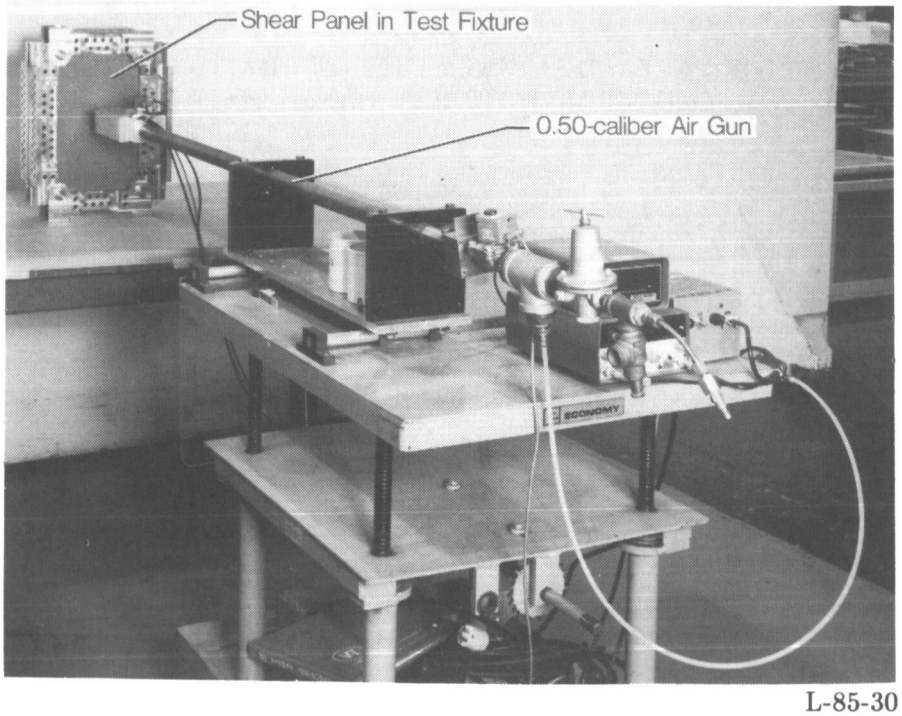

L-85-30

Figure 2. Low-velocity impact test setup.

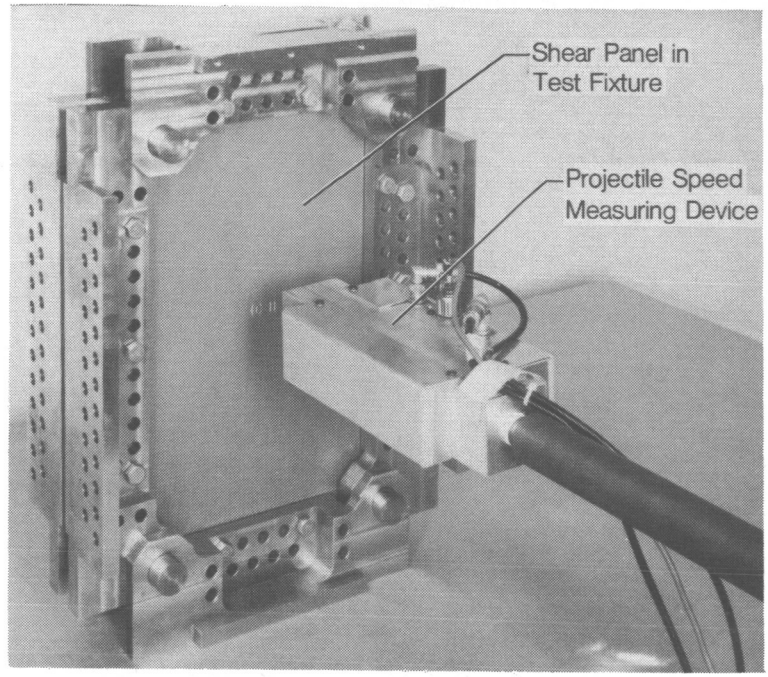

L-85-31

Figure 3. Close-up view of test panel in fixture prior to being impacted.

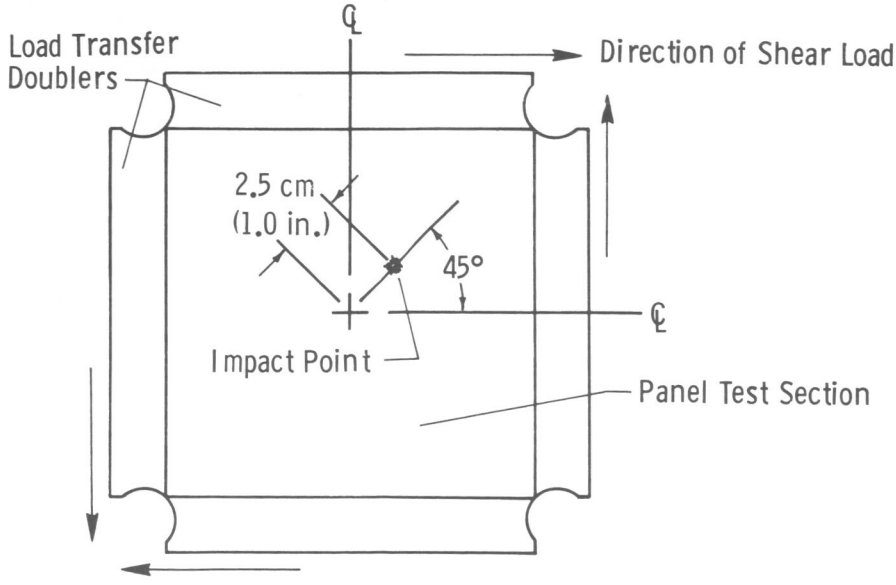

Figure 4. Low-speed impact region for composite shear panels.

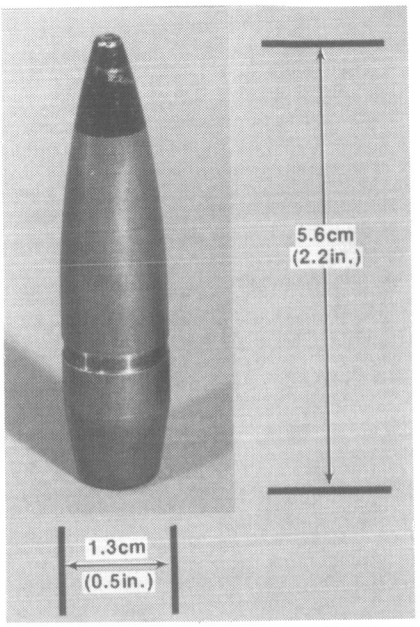

L-85-32

Figure 5. Photo of 0.50-caliber projectile.

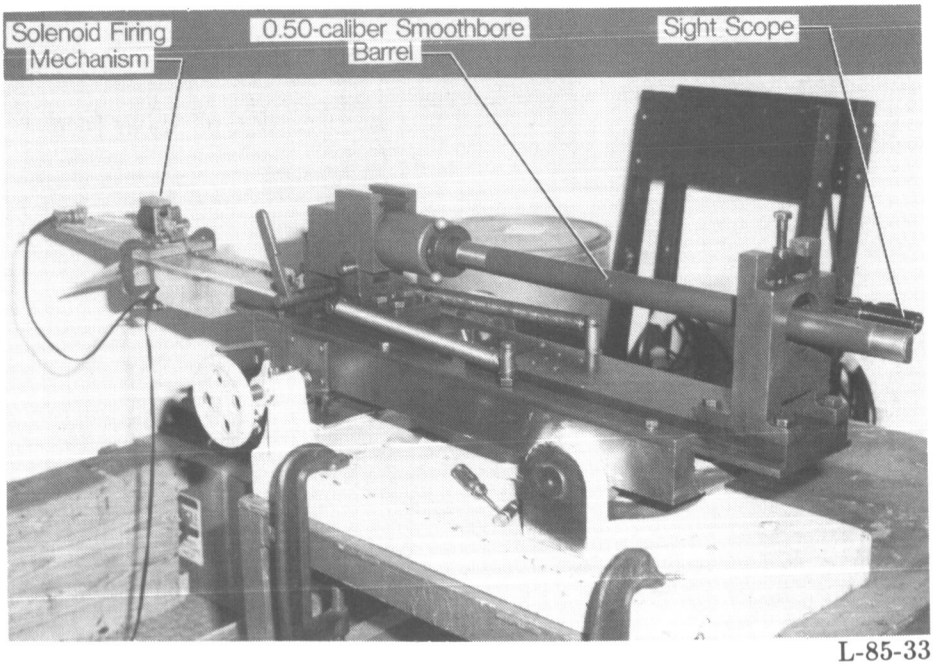

L-85-33

Figure 6. Photo of 0.50-caliber, 76.2-cm (30.0-in.) smoothbore barrel mounted on test stand.

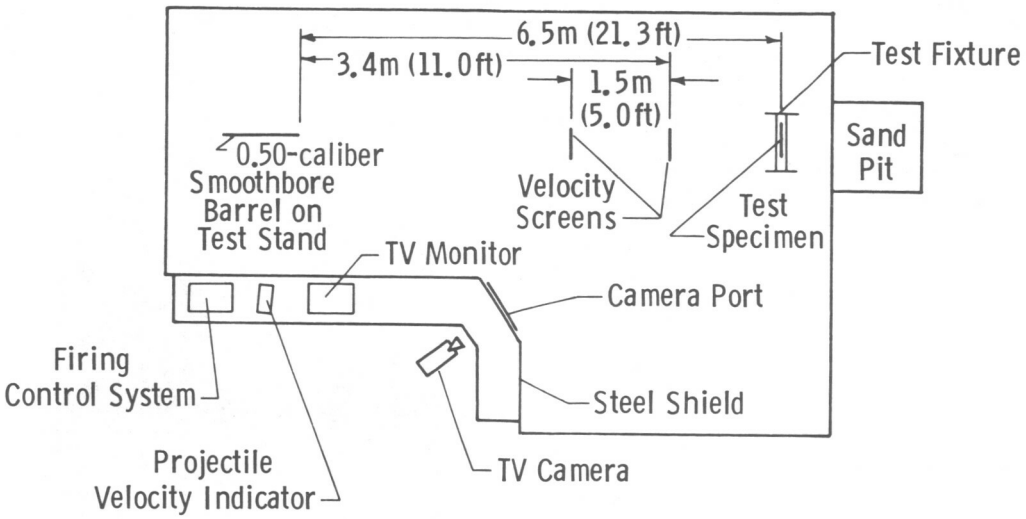

Figure 7. Ballistic impact test firing range with test specimen.

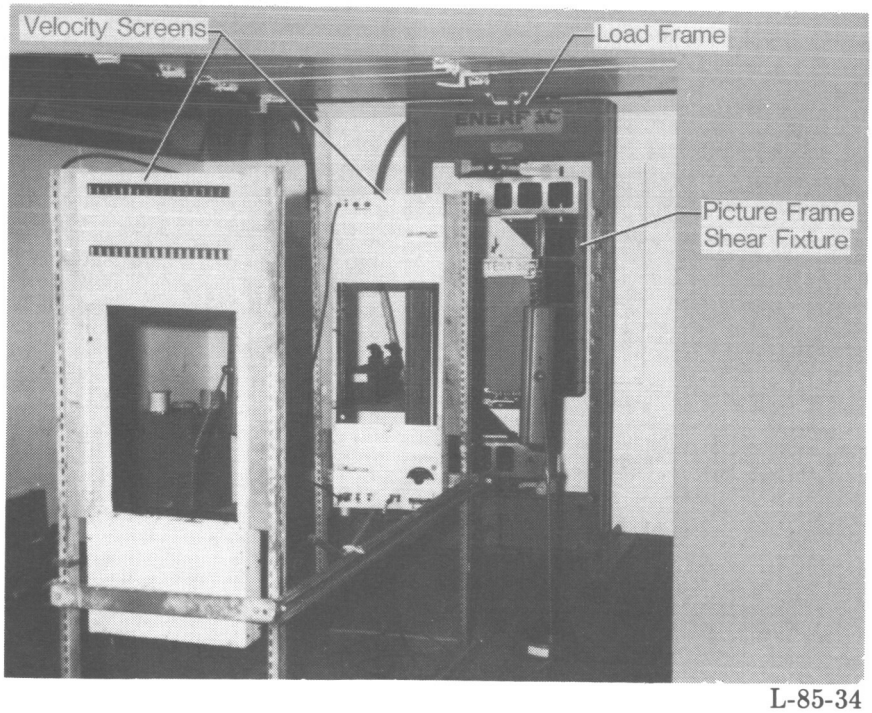

L-85-34

Figure 8. Ballistic impact test apparatus with velocity screens.

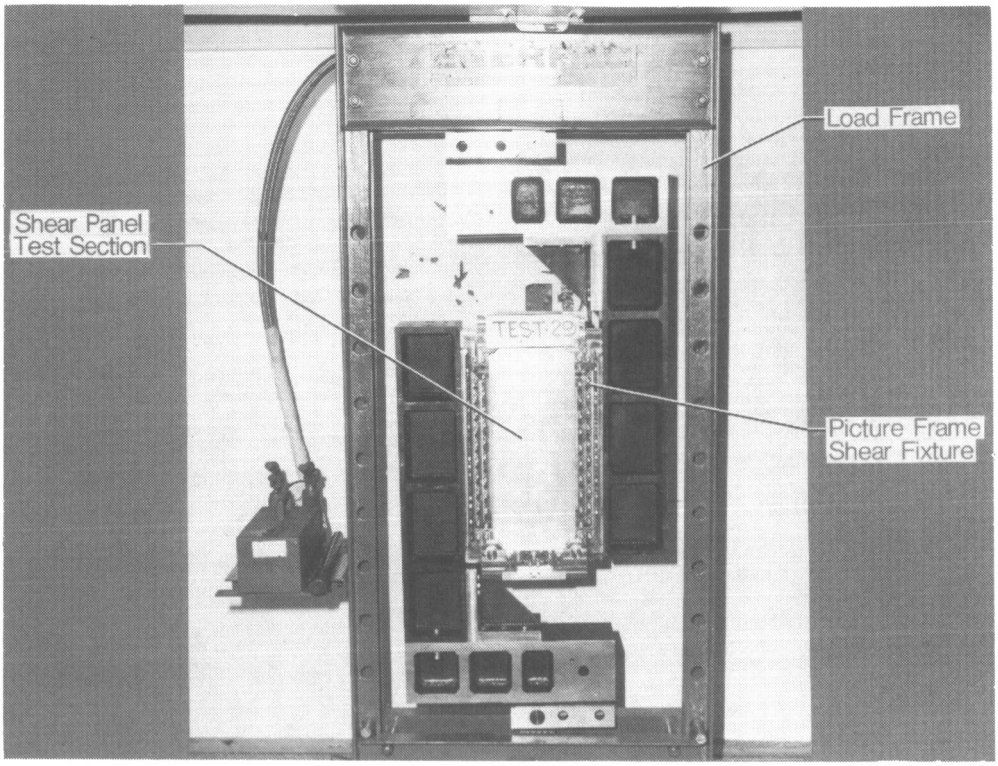

L-85-35

Figure 9. Shear fixture in ballistic impact load frame.

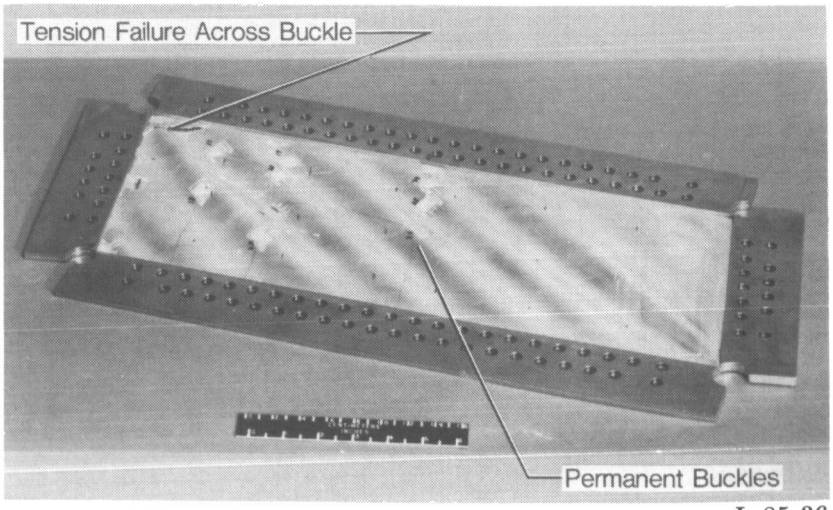

L-85-36

Figure 10. Failed aluminum diagonal tension field shear panel.

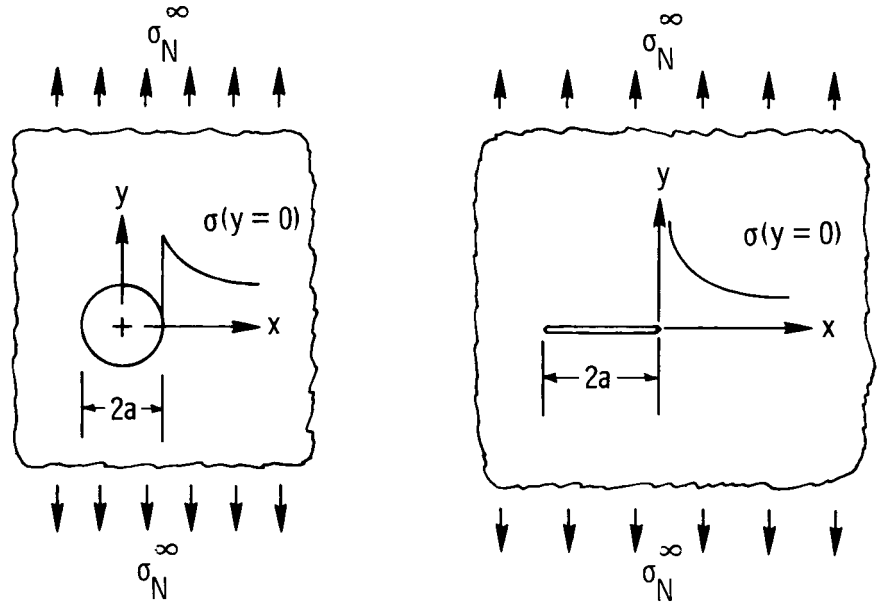

(a) Hole in an infinite plate. (b) Crack in an infinite plate.

Figure 11. Stress distribution about a hole and a crack in infinite plates.

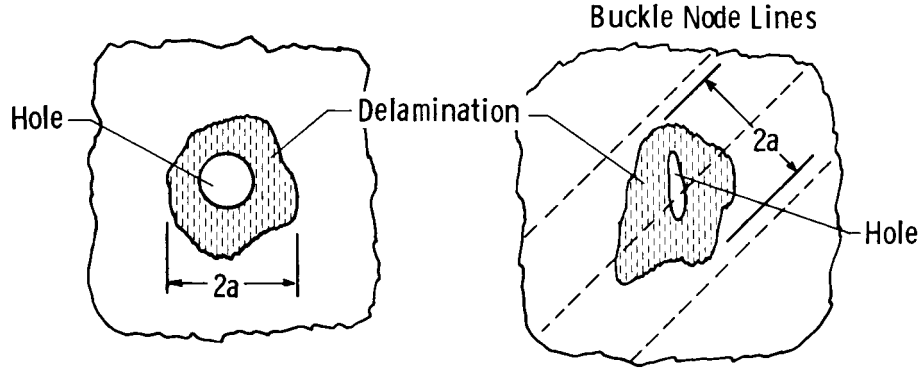

(a) Low-speed impact. (b) Ballistic impact.

Figure 12. Hole diameter and crack length ($2a$) in impacted panels.

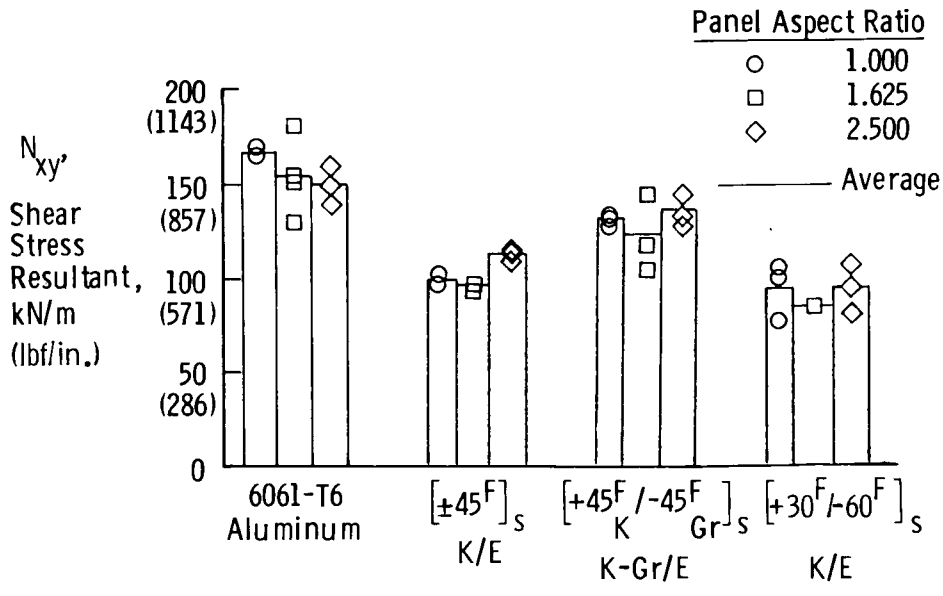

Figure 13. Ultimate shear stress resultants of undamaged panel tests.

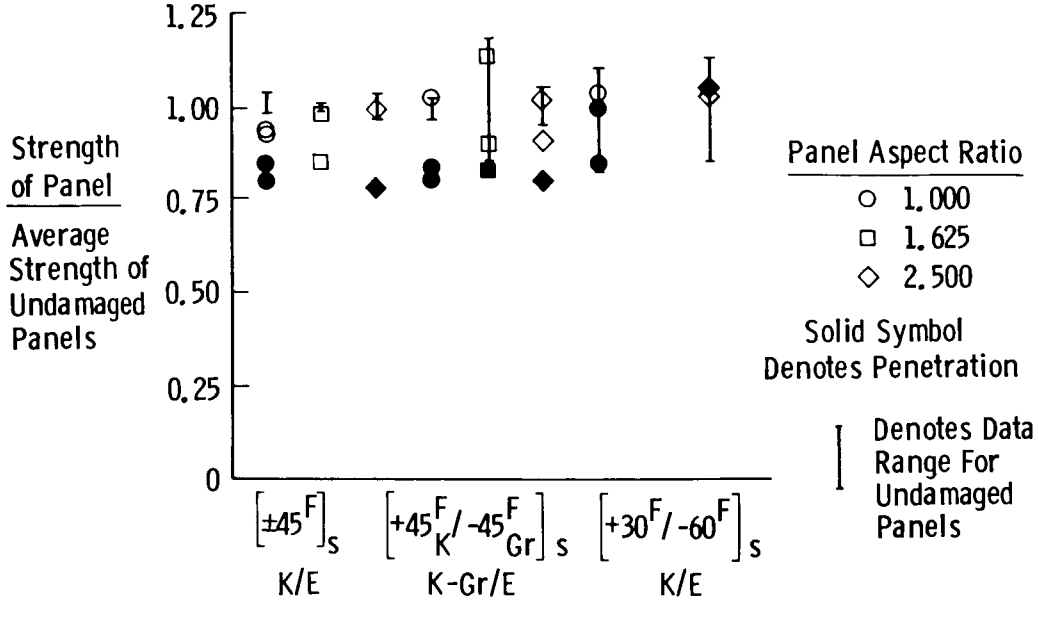

Figure 14. Residual strength ratio of panels impacted at low speed.

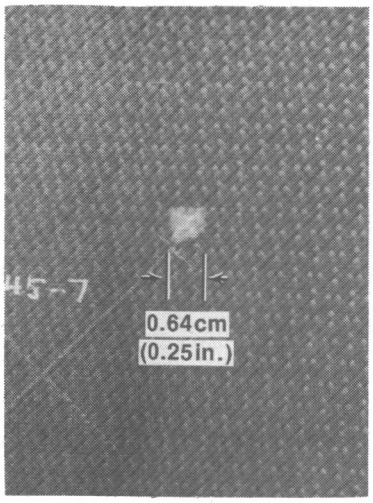

Impacted side

L-85-37

Figure 15. Damaged region of $[+45^{F}_{K}/-45^{F}_{Gr}]_{s}$ K-Gr/E shear panel impacted at 46 m/sec (150 ft/sec).

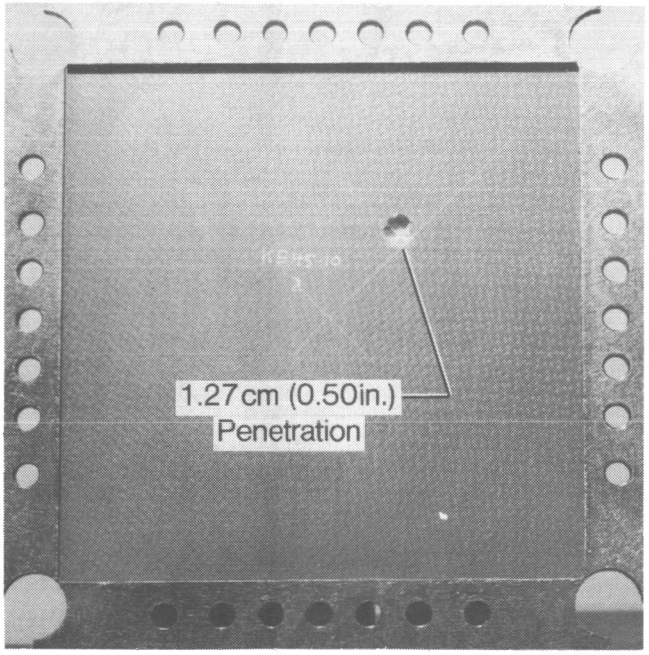

Impacted side

L-85-38

Figure 16. $[\pm 45^{F}]_{s}$ K/E shear panel impacted at 67 m/sec (220 ft/sec).

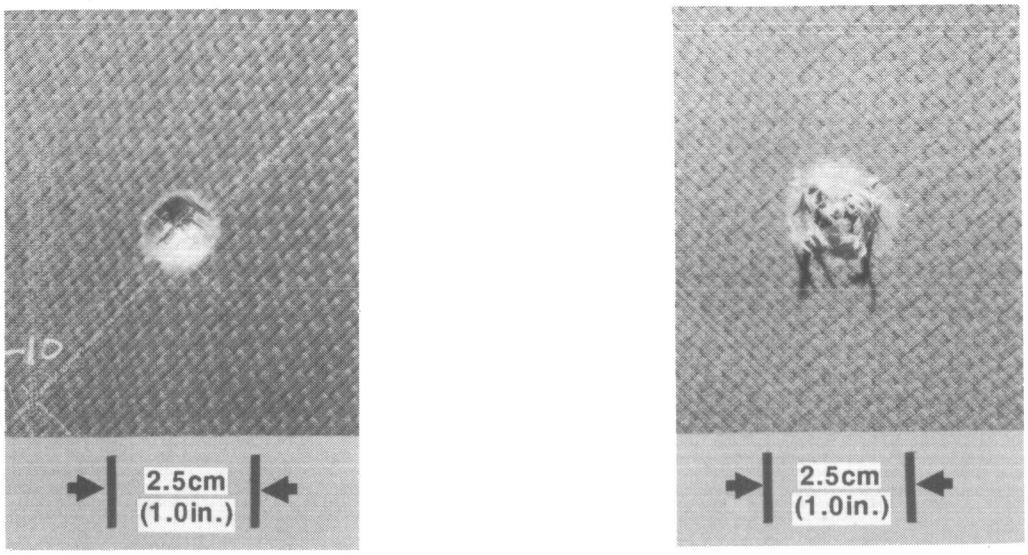

(a) Impacted side.

(b) Exit side.

L-85-39

Figure 17. Damaged region of $[+45^{F}_{K}/-45^{F}_{Gr}]_s$ K-Gr/E shear panel impacted at 67 m/sec (220 ft/sec).

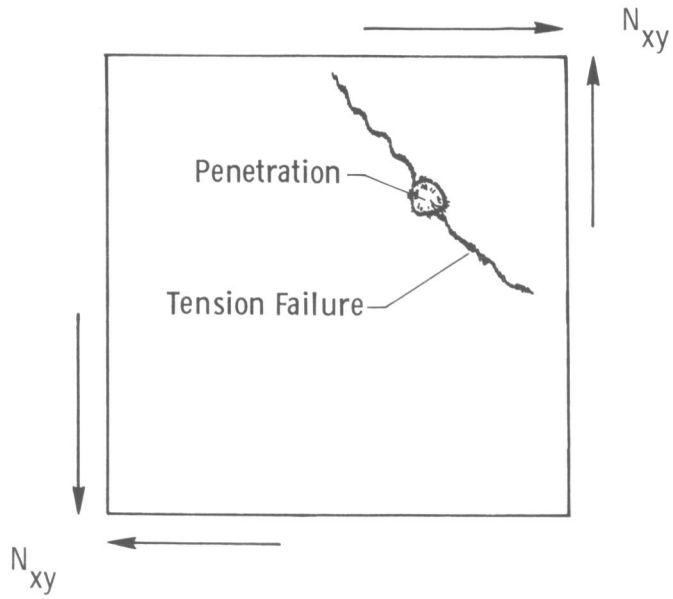

Figure 18. Typical failure mode of $[\pm 45^{F}]_s$ K/E shear panels impacted at 67 m/sec (220 ft/sec).

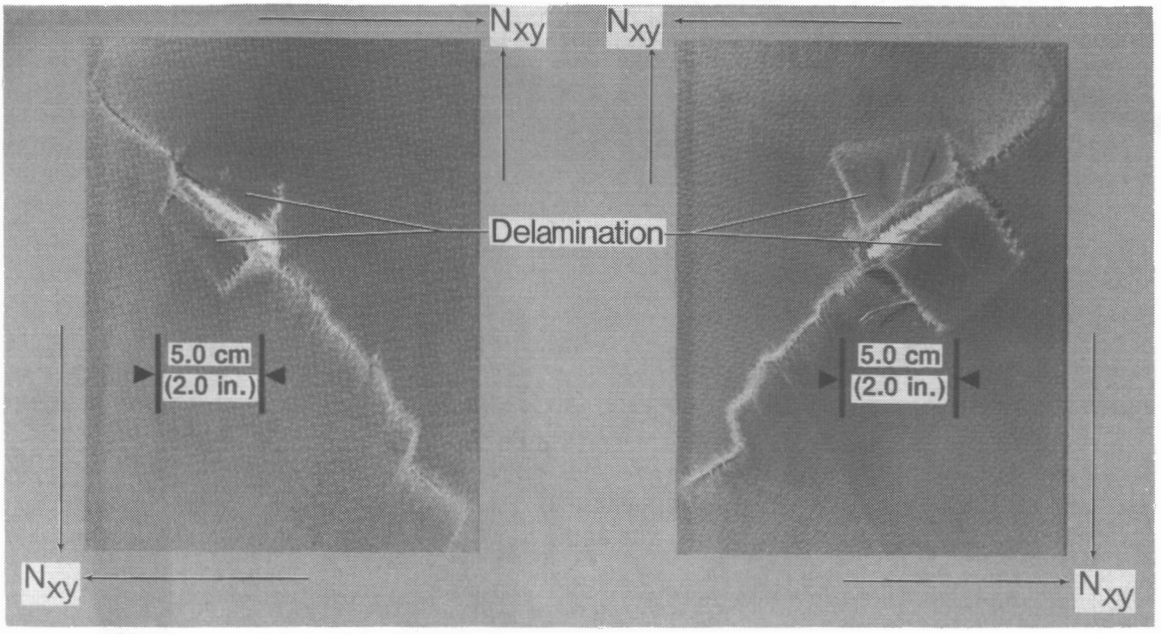

(a) Impacted side. (b) Exit side.

L-85-40

Figure 19. Typical damaged region of ballistically impacted $[\pm 45^{F}]_s$ K/E shear panel. Panel failed upon impact; hole size corresponds to projectile tumble angle of 90°.

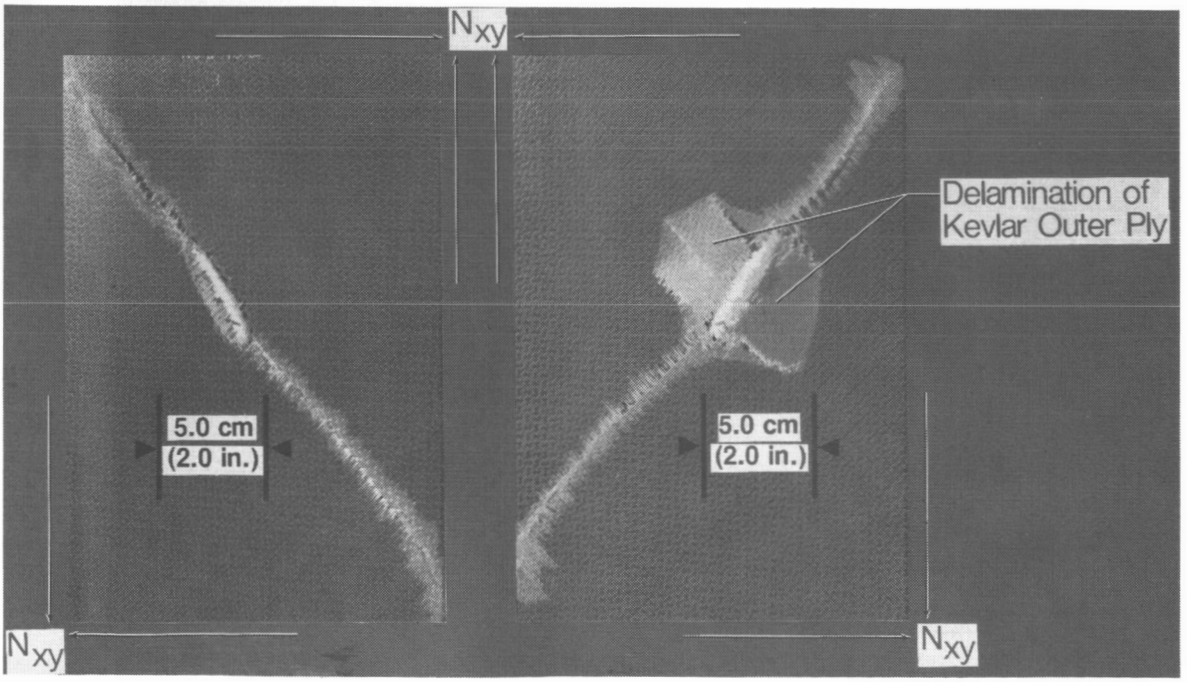

(a) Impacted side. (b) Exit side.

L-85-41

Figure 20. Typical damaged region of ballistically impacted $[+45^{F}_{K}/-45^{F}_{Gr}]_s$ K-Gr/E shear panel. Panel failed upon impact; hole size corresponds to projectile tumble angle of 69°.

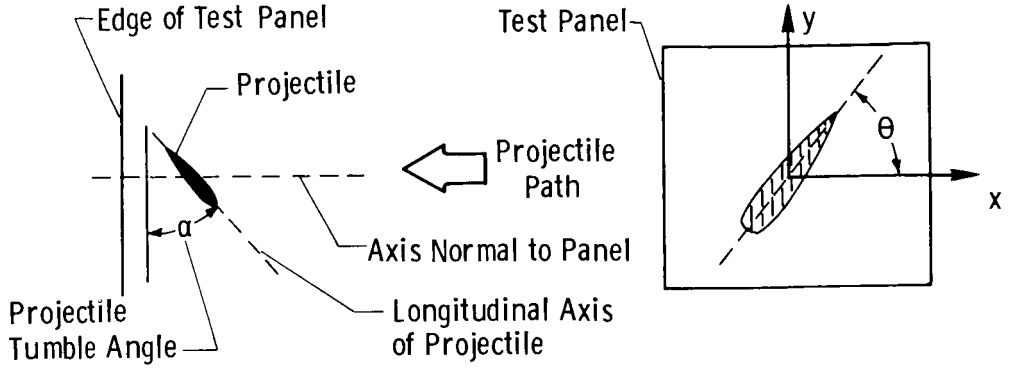

(a) Projectile tumble angle. (b) Projectile orientation angle.

Figure 21. Ballistic projectile tumble and orientation definition.

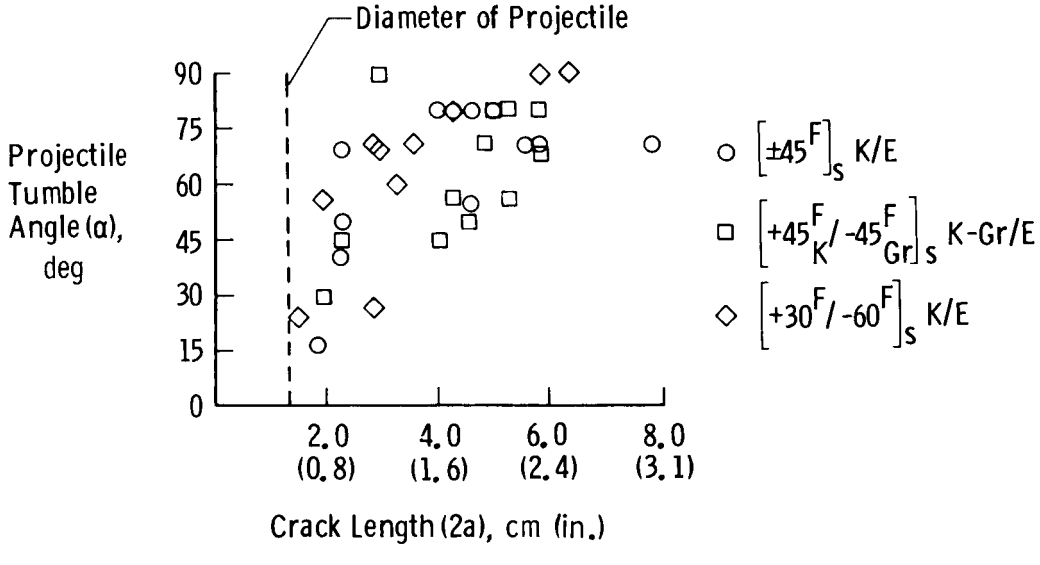

Figure 22. Effect of projectile tumble angle α on crack length.

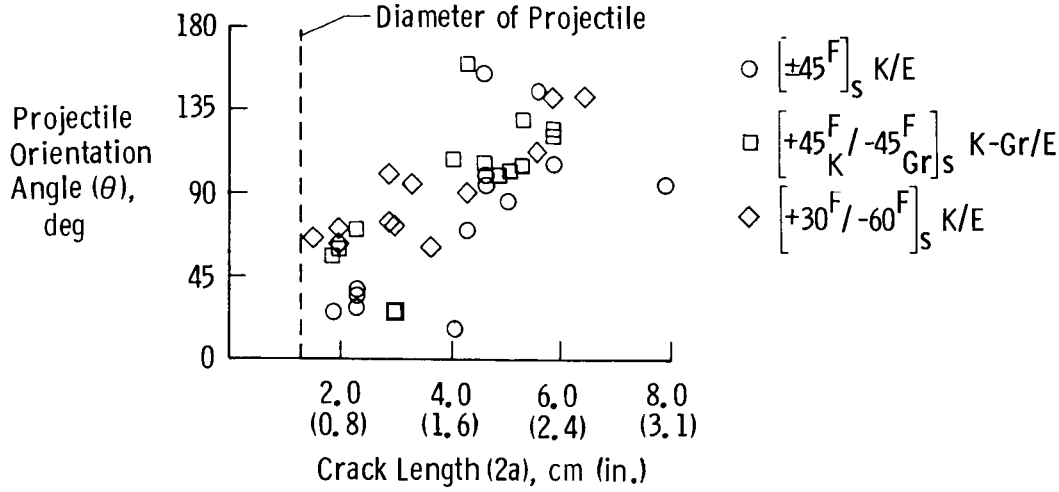

Figure 23. Effect of projectile orientation angle θ on crack length.

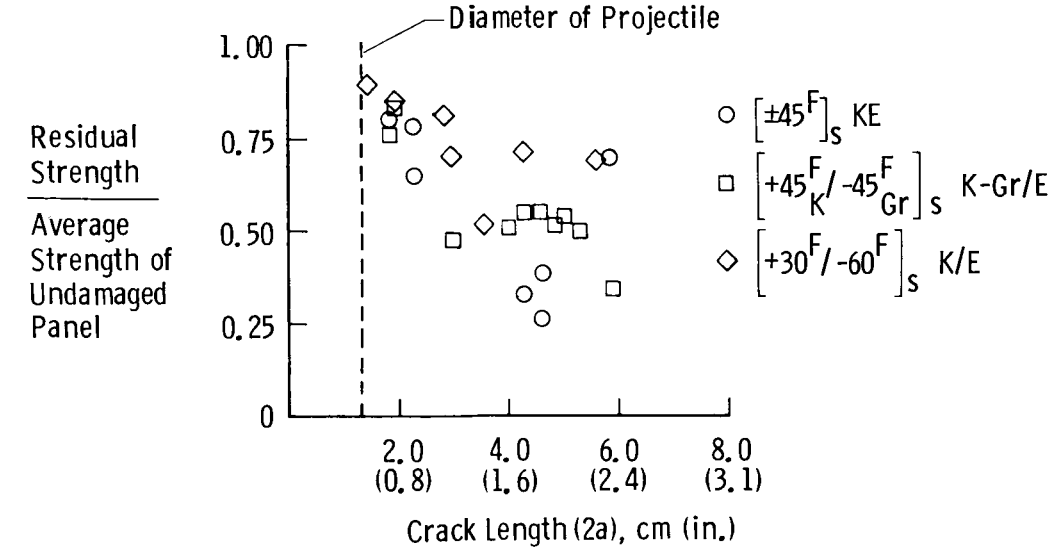

Figure 24. Effect of crack length on residual strength of ballistically impacted panels.

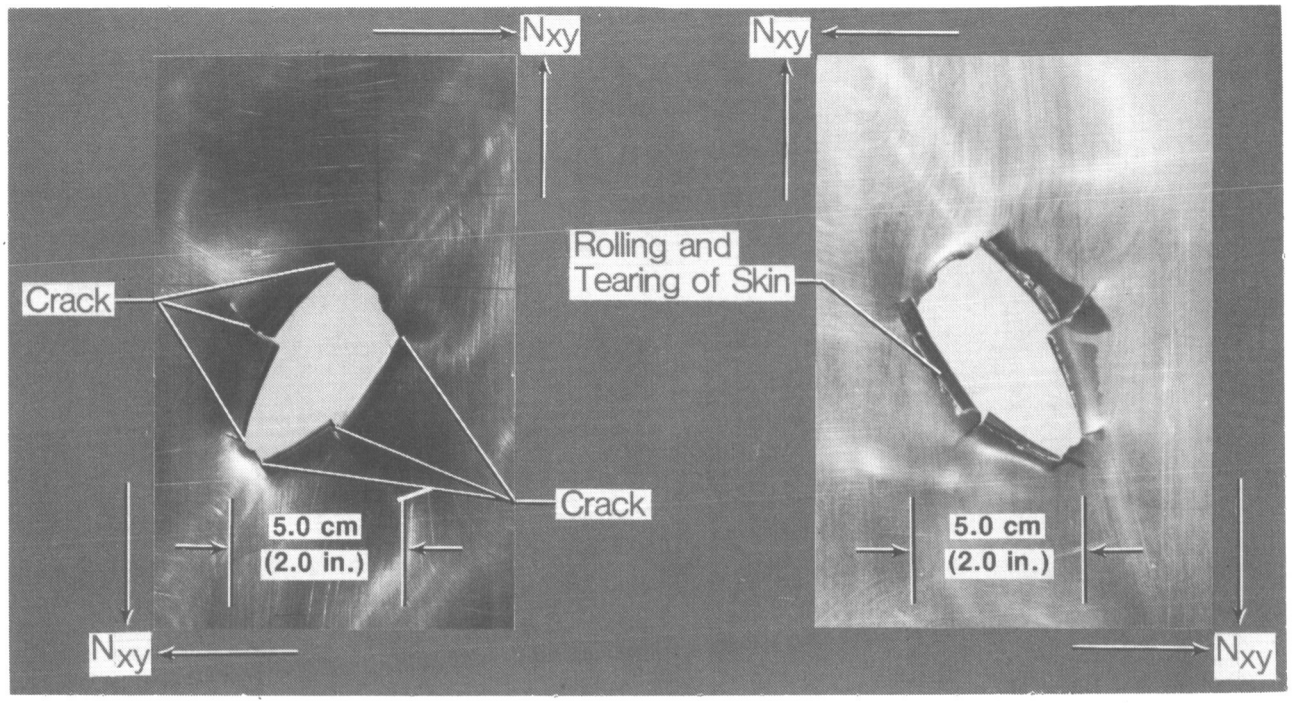

(a) Impacted side. (b) Exit side.

L-85-42

Figure 25. Typical damaged region of ballistically impacted aluminum shear panel. Panel survived impact; hole size corresponds to projectile tumble angle of 90°.

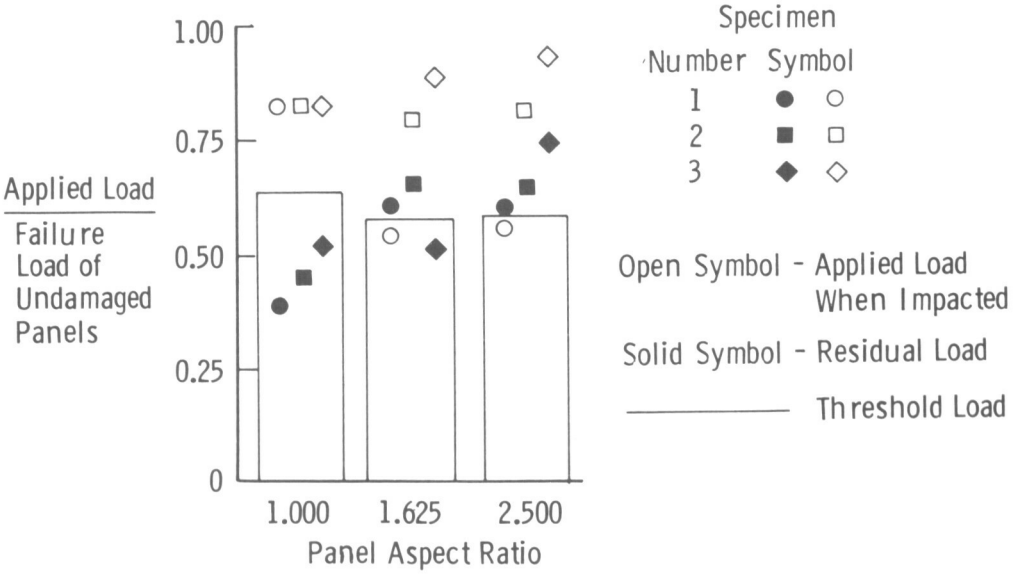

Figure 26. Load ratios of ballistically impacted aluminum panels.

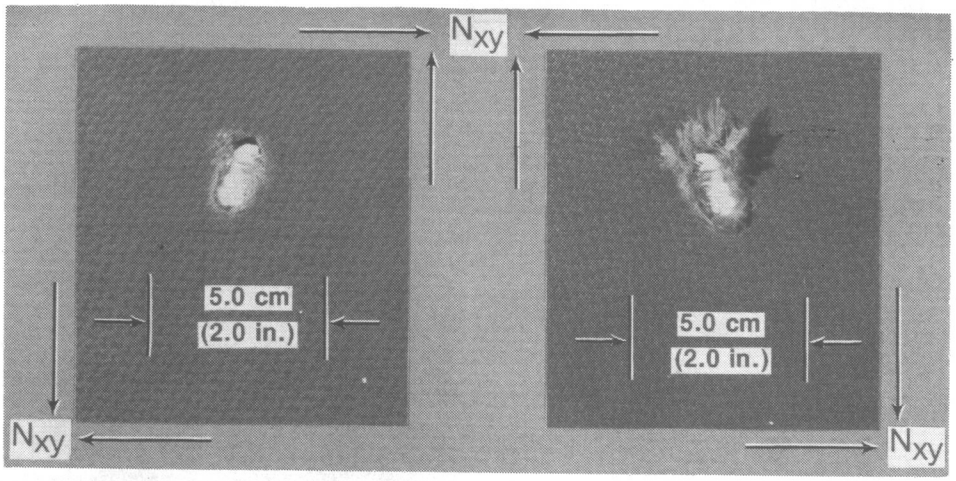

(a) Impacted side. (b) Exit side.

L-85-43

Figure 27. Damaged region of ballistically impacted $[\pm 45^{F}]_s$ K/E shear panel. Panel survived impact; hole size corresponds to projectile tumble angle of 20°.

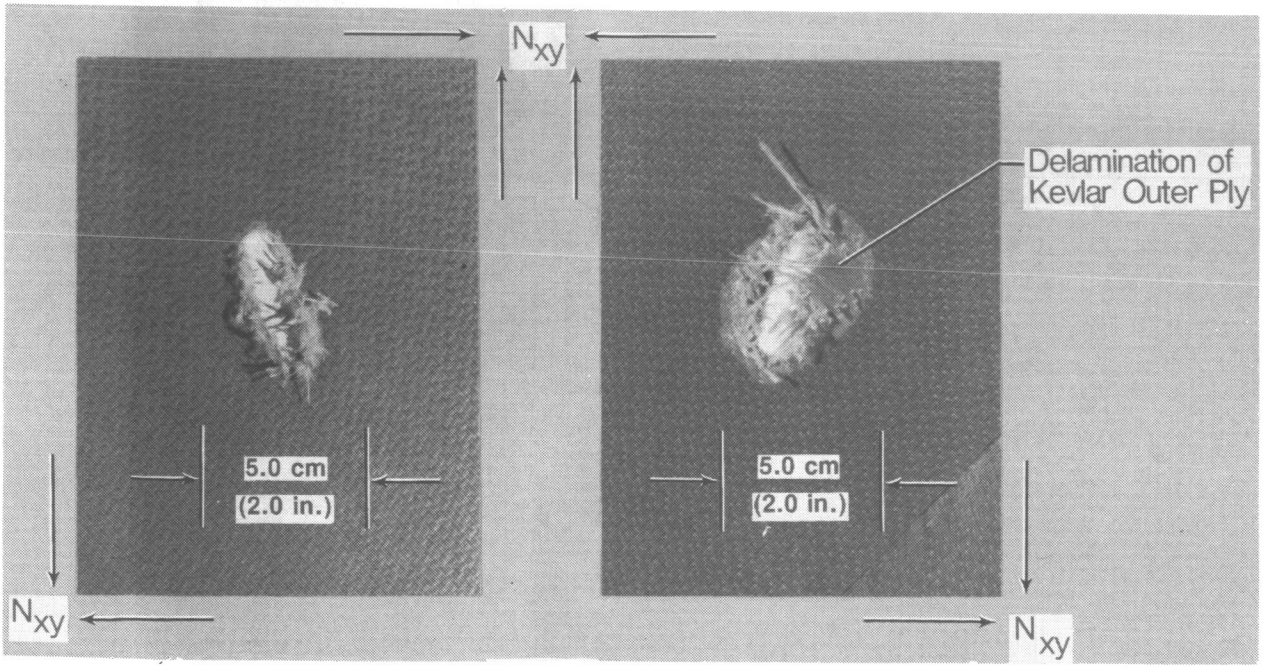

(a) Impacted side. (b) Exit side.

L-85-44

Figure 28. Damaged region of ballistically impacted $[+45^{F}_{K}/-45^{F}_{Gr}]_s$ K-Gr/E shear panel. Panel survived impact; hole size corresponds to projectile tumble angle of 45°.

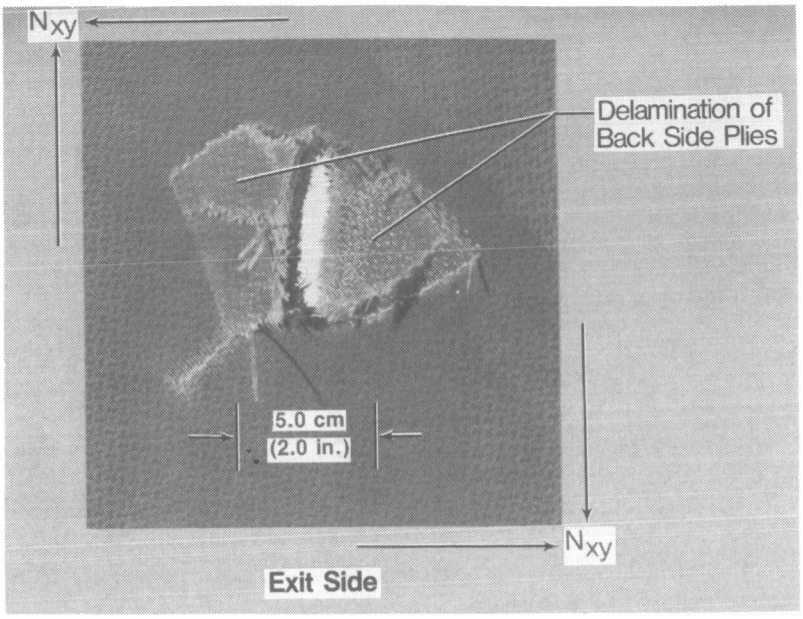

L-85-45

Figure 29. Typical exit side damage of ballistically impacted $[\pm 45^{F}]_s$ K/E shear panel. Panel survived impact; hole size correpsonds to projectile tumble angle of 80°.

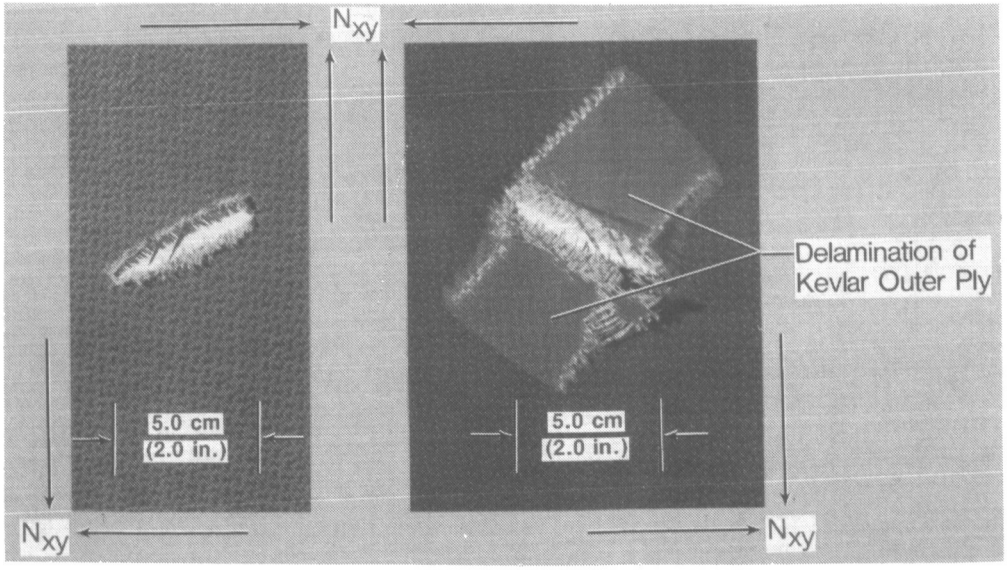

(a) Impacted side. (b) Exit side.

L-85-46

Figure 30. Typical damaged region of ballistically impacted $[+45^{F}_{K}/-45^{F}_{Gr}]_s$ K-Gr/E shear panel. Panel survived impact; hole size corresponds to projectile tumble angle of 90°.

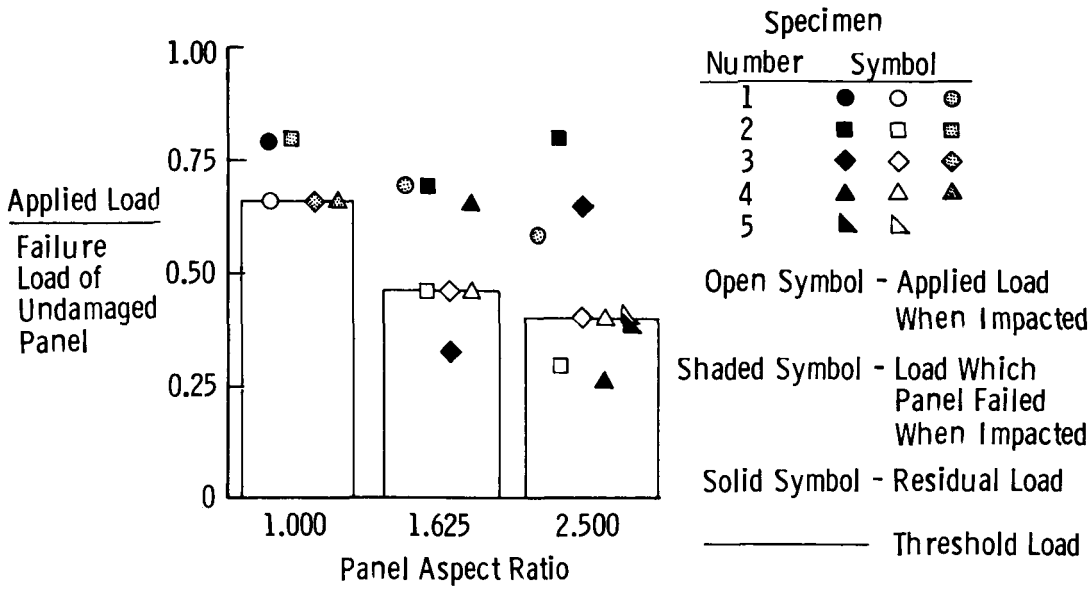

Figure 31. Load ratios of $[\pm 45^{F}]_s$ K/E ballistically impacted composite panels.

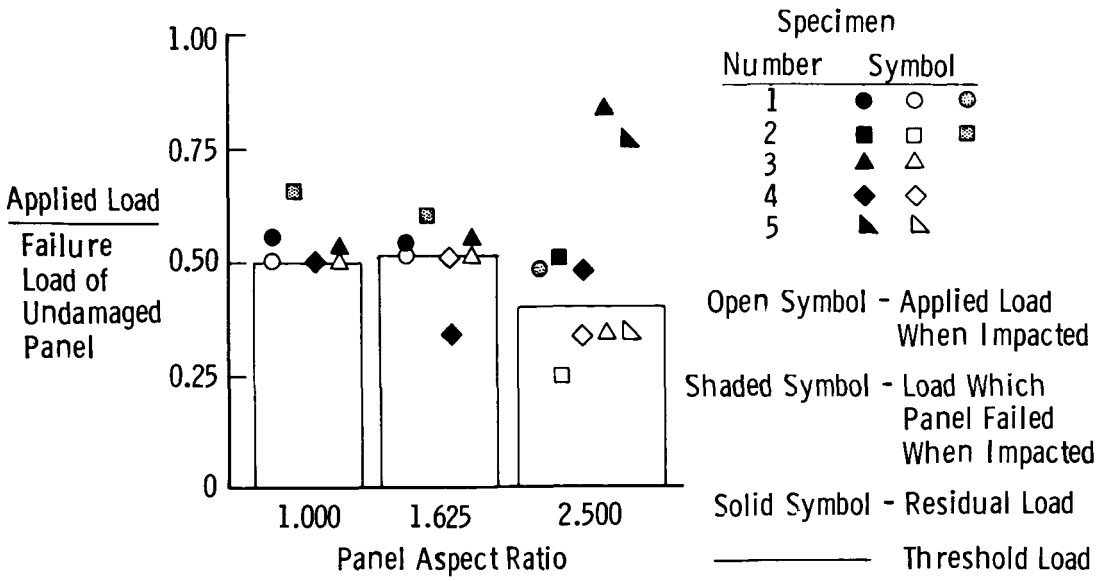

Figure 32. Load ratios of $[+45^{F}_{K}/-45^{F}_{Gr}]_s$ K-Gr/E ballistically impacted composite panels.

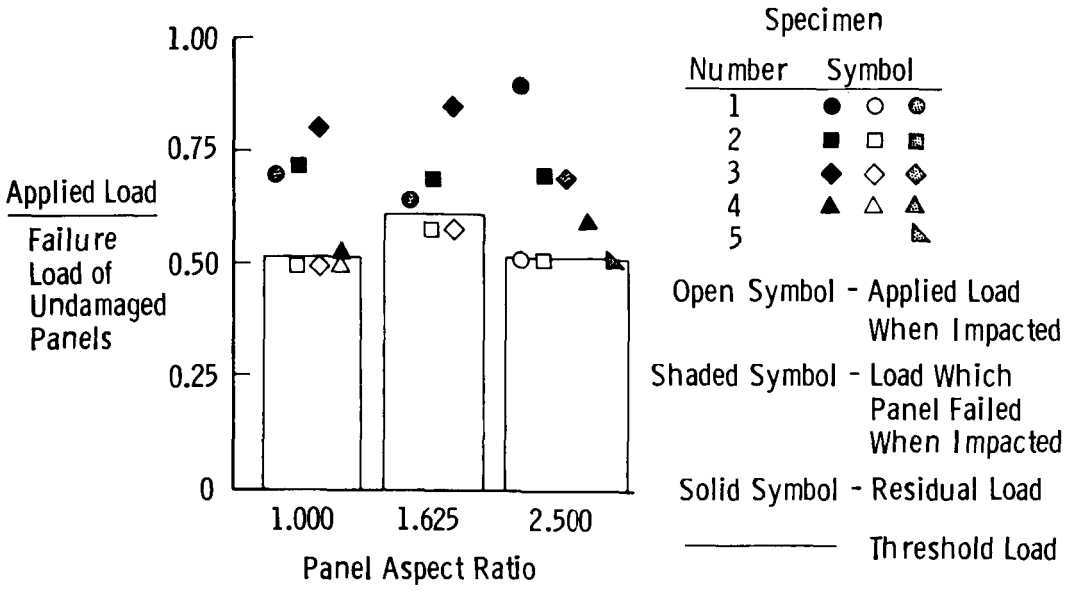

Figure 33. Load ratios of $[+30^F/-60^F]_s$ K/E ballistically impacted composite panels.

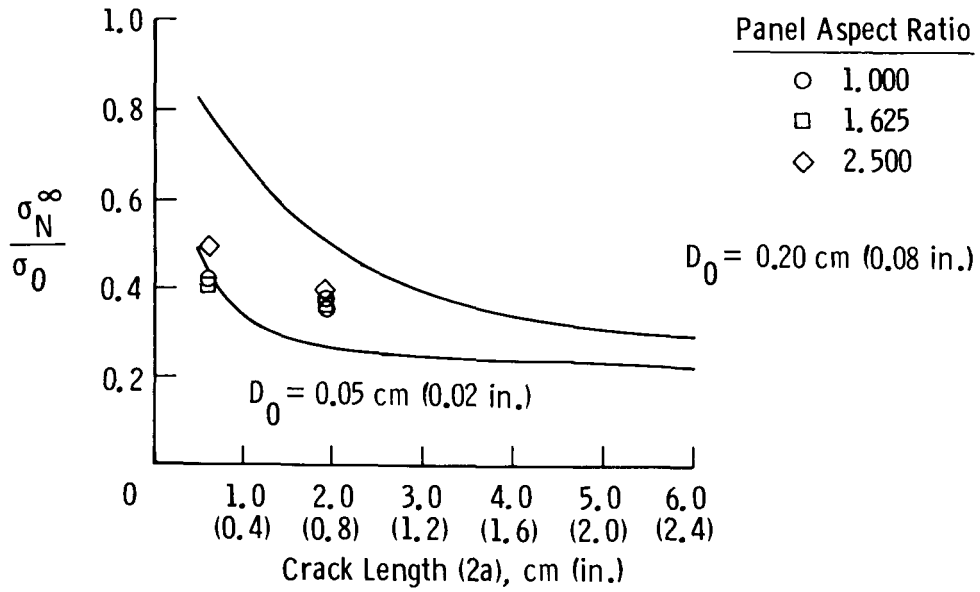

Figure 34. Point stress criteria for $[\pm 45^F]_s$ K/E shear panel impacted at low velocity.

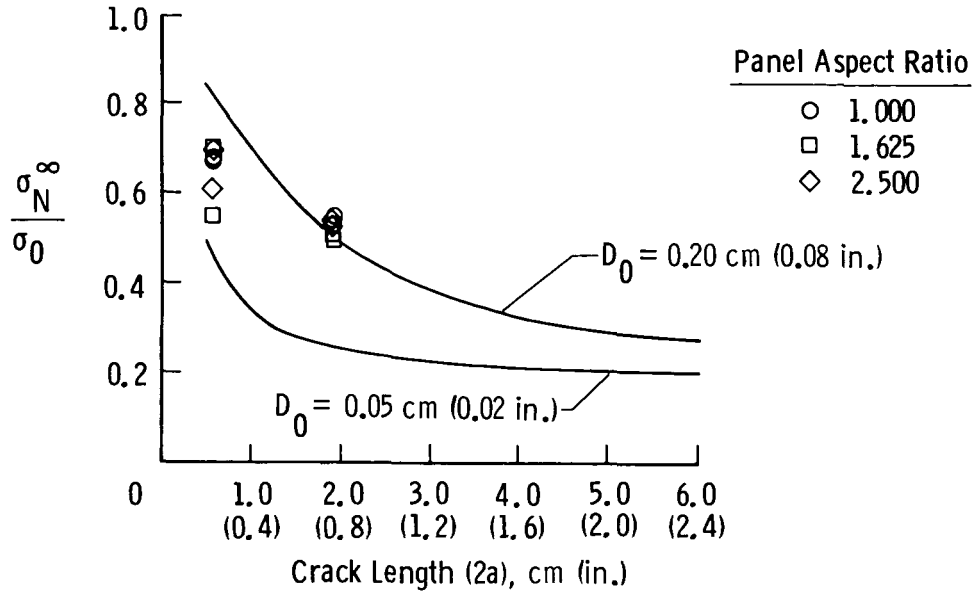

Figure 35. Point stress criteria for $[+45_K^F/-45_{Gr}^F]_s$ K-Gr/E shear panel impacted at low velocity.

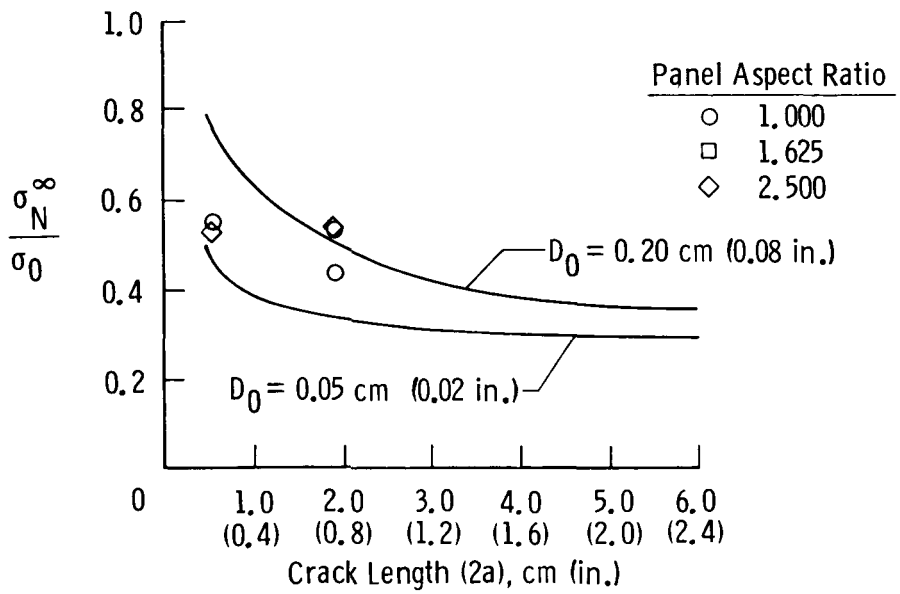

Figure 36. Point stress criteria for $[+30^F/-60^F]_s$ K/E shear panel impacted at low velocity.

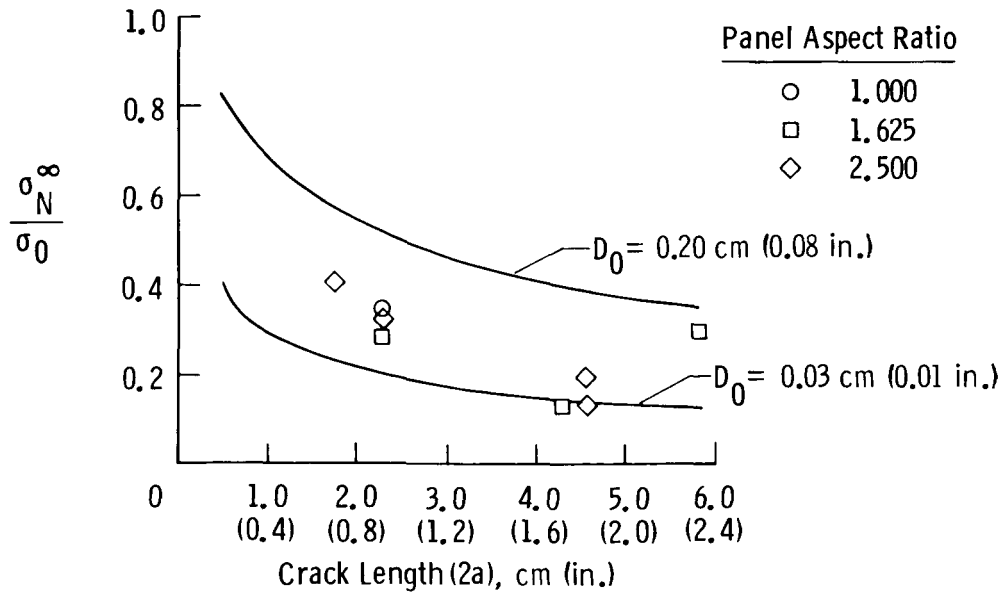

Figure 37. Point stress criteria for ballistically impacted $[\pm 45^F]_s$ K/E shear panel.

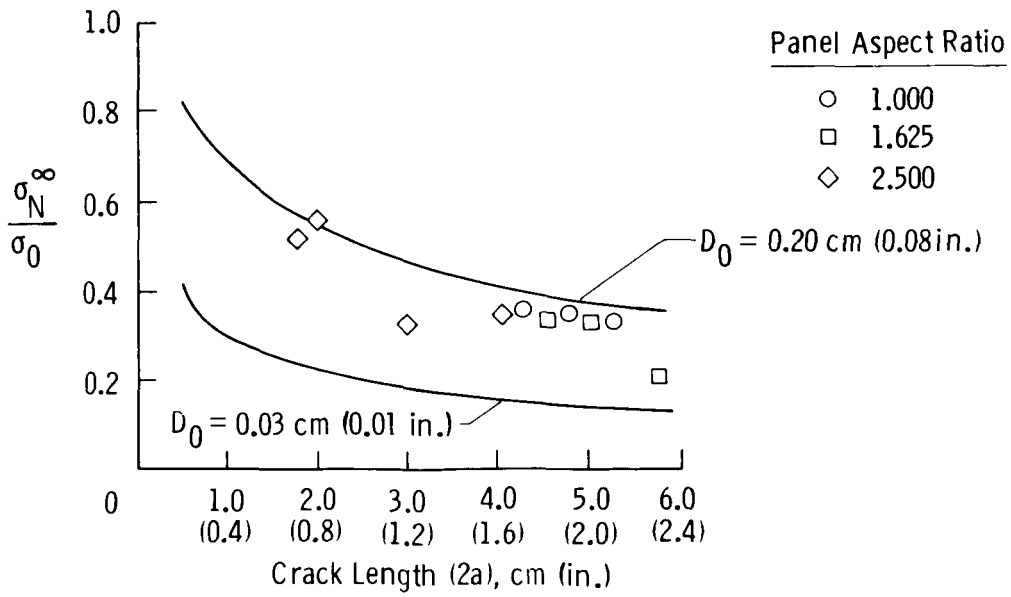

Figure 38. Point stress criteria for ballistically impacted $[+45_K^F/-45_{Gr}^F]_s$ K-Gr/E shear panel.

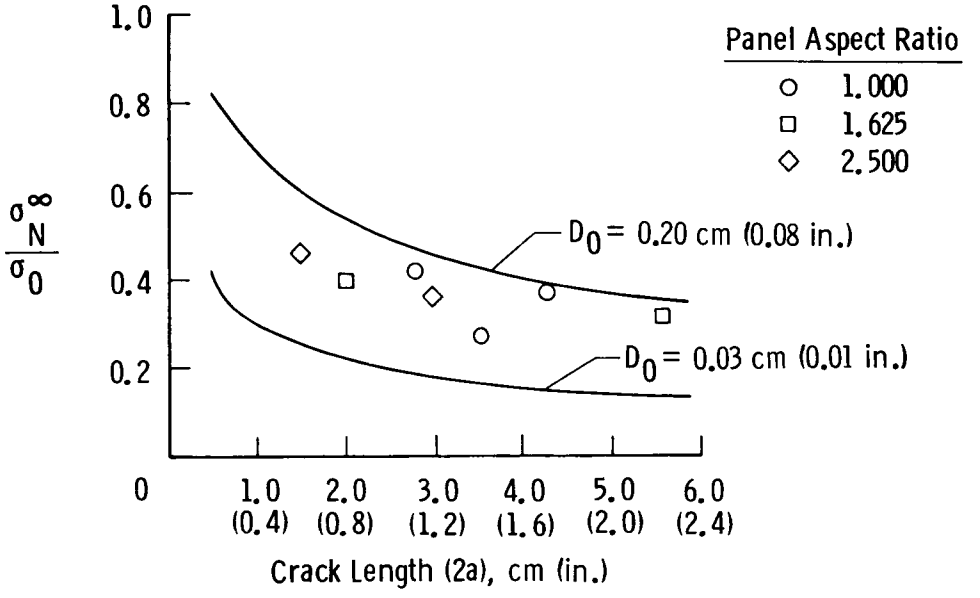

Figure 39. Point stress criteria for ballistically impacted $[+30^F/-60^F]_s$ K/E shear panel.

1. Report No.	2. Government Accession No.	3. Recipient's Catalog No.
NASA TP-2441 AVSCOM TR 85-B-1		

4. Title and Subtitle	5. Report Date
Effect of Low-Velocity or Ballistic Impact Damage on the Strength of Thin Composite and Aluminum Shear Panels	May 1985
	6. Performing Organization Code: 505-42-23-03
7. Author(s): Gary L. Farley	8. Performing Organization Report No.: L-15942
9. Performing Organization Name and Address: Structures Laboratory, USAAVSCOM Research and Technology Laboratories, NASA Langley Research Center, Hampton, VA 23665	10. Work Unit No.
	11. Contract or Grant No.
12. Sponsoring Agency Name and Address: National Aeronautics and Space Administration, Washington, DC 20546 and U.S. Army Aviation Systems Command, St. Louis, MO 63120	13. Type of Report and Period Covered: Technical Paper
	14. Army Project No.: 1L161102.H4503

15. Supplementary Notes

Gary L. Farley: Structures Laboratory, USAAVSCOM Research and Technology Laboratories.

16. Abstract

Impact tests were conducted on shear panels fabricated from 6061-T6 aluminum and from woven-fabric prepreg of Du Pont Kevlar fiber/epoxy resin and graphite fiber/epoxy resin. The shear panels consisted of three different composite laminates and one aluminum material configuration. Three panel aspect ratios were evaluated for each material configuration. Composite panels were impacted with a 1.27-cm (0.05-in.) diameter aluminum sphere at low velocities of 46 m/sec (150 ft/sec) and 67 m/sec (220 ft/sec). Ballistic impact conditions consisted of a tumbled 0.50-caliber projectile impacting loaded composite and aluminum shear panels. The results of these tests indicate that ballistic threshold load (the lowest load which will result in immediate failure upon penetration by the projectile) varied between 0.44 and 0.61 of the average failure load of undamaged panels. The residual strengths of the panels after ballistic impact varied between 0.55 and 0.75 of the average failure strength of the undamaged panels. The low-velocity impacts at 67 m/sec (220 ft/sec) caused a 15- to 20-percent reduction in strength, whereas the impacts at 46 m/sec (150 ft/sec) resulted in negligible strength loss. Good agreement was obtained between the experimental failure strengths and the predicted strength with the point stress failure criterion.

17. Key Words (Suggested by Authors(s))	18. Distribution Statement
Composite materials Shear panels Damage tolerance Low-velocity impact Ballistic damage Postbuckling Helicopter Fuselage	Unclassified—Unlimited Subject Categories 24, 39

19. Security Classif.(of this report)	20. Security Classif.(of this page)	21. No. of Pages	22. Price
Unclassified	Unclassified	39	A03

For sale by the National Technical Information Service, Springfield, Virginia 22161

NASA-Langley, 1985

National Aeronautics and
Space Administration

Washington, D.C.
20546

Official Business
Penalty for Private Use, $300

THIRD-CLASS BULK RATE

Postage and Fees Paid
National Aeronautics and
Space Administration
NASA-451

NASA

POSTMASTER: If Undeliverable (Section 158 Postal Manual) Do Not Return